Waste Management Bulletin 2 (2024) 275–288

Contents lists available at ScienceDirect

Waste Management Bulletin

journal homepage: www.elsevier.com/locate/wmb

Investigation of hydrohalic acids as lixiviants for the leaching of cathode metals from spent lithium-ion batteries

Prichard M. Tembo, Vaidyanathan Subramanian *

Department of Chemical and Materials Engineering, University of Nevada-Reno, 1664 N. Virginia Street, Reno, Nevada 89557, USA

ARTICLE INFO

Keywords:
Leaching
Lithium-ion batteries
Recycling
Shrinking-core model
Kinetics

ABSTRACT

The exploration of alternative energy sources is inextricably linked with energy storage considerations. Current high density energy storage options on the market rely heavily on lithium (Li)-based technologies. A projected increase in energy storage technology demand has sounded the alarm on a need to develop suitable approaches for the recovery of the various constituent metals from spent Li-ion batteries (LIBs). This, coupled with urgent consideration for the environment has necessitated the investigation of various LIB metal recovery techniques. In this work, we explore the novel application of the hydrohalic acids, hydrobromic (HBr) and hydroiodic (HI) acid, as lixiviants in a series of leaching experimental investigations on LIB cathode powder. A methodology for battery disassembly and cell cathode material recovery is presented leading up to the metal leaching. Our results indicate that the lixiviants can be utilized in the absence of a reducing agent which is typically present in conventional LIB leaching systems. The highest recoveries of the constituent metals, Co, Li, Mn and Ni in the HI system were 92.9 %, 93.6 %, 93.1 % and 94.5 % respectively, at an operating temperature of 60 ℃ and with a 1.5 M HI concentration. The HBr system achieved metal recoveries of 90.6 %, 89.1 %, 83.1 % and 96.4 % for Co, Li, Mn and Ni respectively, at 60 ℃ and using 2 M HBr. Kinetic studies showed that the leaching mechanism for both acids follow a chemical reaction-controlled model.

Introduction

The discussion around fully leveraging renewable energy technologies is one that has been synonymous with energy storage concerns. Technological advancements focusing on portable devices and electrical transportation such as electrical vehicles (EVs) have further spurred on studies into improving energy storage technologies (Wei et al., 2017; Berckmans et al., 2017; Harper et al., 2019; Mo and Jeon, 2018). Energy storage technologies involving lithium (Li) as the platform [lithium batteries (LBs) and lithium-ion batteries (LIBs)], which offer a high energy density, are long lasting and environmentally friendly (Duan et al., 2020; Zhou et al., 2018), have been widely adopted. These technologies feature a number of chemistries comprised of different key elements such as cobalt (Co), nickel (Ni), manganese (Mn) and iron (Fe), aside from Li (Nadimi and Karazmoudeh, 2021; Bhandari and Dhawan, 2022; Ryu et al., 2021; Li et al., 2019). Proliferation of Li-based technologies has also been largely driven by the vast amount of research and development invested in improving the technologies, which has also resulted in making them cost effective for commercialization over the years (Ziegler et al., 2021; Philippot et al., 2019). Representative figures adapted from work by Ziegler and Trancik (2021), outlining the percentage decrease in lithium-ion cell prices of various cell types, are given in Fig. 1. The figure shows a considerable decrease of ~73–93 % in the cost of Li-based battery products over a span of 27 years. As a result, the growing application of such technologies has led to an increase in demand for the LIB constituent materials.

Predictions show a global LIB demand of 2400 GWh by 2030 and various predicted LIB demand levels by 2040 based off various socio-economic pathway framework models (Degen et al., 2023). The socio-economic pathway framework outlines various possible futures for humanity up until the year 2100 (Riahi et al., 2017). The models that apply to LIBs chiefly focus on three possible pathways: the i) fossil fuel dominant (SEP1), ii) middle way (SEP2) and iii) sustainable (SEP3) pathway (Marscheider-Weidemann et al., 2021). The predicted LIB demand and percentage LIB demand growth between 2030 and 2040 based on each of the three highlighted pathways is given in Table 1. Such predicted growth rate, especially for the SEP3 model, will require a large amount of LIB raw materials. Several of the key LIB constituent

* Corresponding author.
E-mail address: ravisv@unr.edu (V. Subramanian).

https://doi.org/10.1016/j.wmb.2024.08.007

Available online 28 August 2024

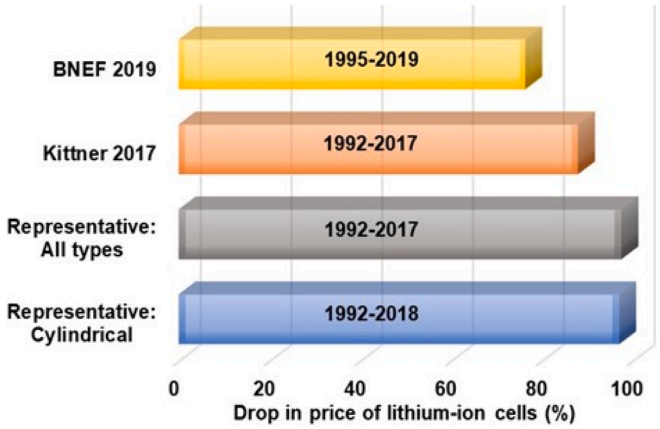

Fig. 1. Percentage decline in lithium-ion cell prices for different cell types over specific time periods (.
adapted from Ziegler and Trancik (2021))

Table 1
Predicted 2040 LIB demand and growth between 2030 and 2040 based on the socioeconomic pathway framework (Degen et al., 2023).

	SEP1	SEP2	SEP3
Predicted 2040 global LIB demand/(GWh)*	2 900	3 400	6 100
Percent increase (2030–2040) in LIB demand/(%)	21	42	154

* Taking into consideration a mixed battery market with new, post lithium-ion battery types.

materials, primarily the cathode metals, have an imbalanced geographical distribution which draws in aspects of geopolitics ad global supply chain concerns (Manjong et al., 2024). For example, a large portion of the world's Co is chiefly mined in the geopolitically unstable Democratic Republic of Congo region, whereas the distribution of extractable Li is also greatly polarized (Tembo et al., 2024; Yu et al., 2022). Apart from the demand for raw materials, increased LIB uptake will consequently result in large volumes of waste LIBs that would require treatment at their end of life (EoL). It is estimated that by 2030 an upward of 5 million tons of LIBs will be at EoL (Quebec, 2019). The combined need for alternative sources for LIB constituent materials and approaches for addressing EoL LIBs has necessitated studies focusing on the recovery and re-use of the different LIB constituents (Tembo et al., 2024; Yang et al., 2017). Recycling has emerged as a possible solution for supplementing the supply of much needed LIB constituent materials while simultaneously providing a means for handling LIB waste (Tembo et al., 2024; Abdalla et al., 2023).

Various process approaches addressing the recycling of LIB constituents have been developed with application of different treatment procedures (Sommerville et al., 2020; Huang et al., 2018; Saleem et al., 2023). These LIB recycling approaches can be broadly divided into direct and indirect recycling, while indirect recycling can be further subdivided into pyrometallurgical and hydrometallurgical treatment procedures (Tembo et al., 2024). Mechano-chemical processing may be included as a pretreatment step in either direct or indirect recycling (Tembo et al., 2024). Focusing on indirect recycling, mechano-chemical treatment has mostly been used prior to conducting pyrometallurgical and hydrometallurgical treatment procedures. Mechano-chemical treatment is associated with comminution operations that result in mechanically induced changes in the material which consequently influences the material chemical and physical properties (Yang et al., 2017). Through a combination of mechanical forces such as impact, friction and collision, a portion of the applied mechanical energy is converted into internal energy which improves the material chemical reaction activity and simultaneously changes the material physiochemical properties (Tan and Li, 2015; Beyer and Clausen-Schaumann, 2005; Wang et al., 2018). The main processes that have been highlighted to occur during mechano-chemical treatment are chemical reaction, polymorphic transformations and bond breakage, which all result in an increase in reaction activity and a decrease in activation energy (Maghsoudlou et al., 2016). Pyrometallurgical processes utilize substantially elevated temperatures for the selective extraction and separation of metals or other compounds. They produce negligible to no liquid waste which allows for scale up and large-scale processing of materials and as a result, they are mostly applied at commercial scale (Makuza et al., 2021; Zhou et al., 2021). Major drawbacks associated with the pyrometallurgical techniques include pollutant generation as well as high energy demand (Liu et al., 2019; Yadav et al., 2020).

In contrast to pyrometallurgical techniques, two significant benefits of the hydrometallurgical processing route are: i) this approach offers relatively less pollutant generation and ii) has a lower energy demand making the process a very promising one from a sustainability standpoint (Lv et al., 2018; Chan et al., 2021). Hydrometallurgical techniques are utilized in conventional metal production processes (well-known and thoroughly investigated) (Guo et al., 2019; Guo et al., 2017; Rosales et al., 2016; Amer, 2008; Yan et al., 2012; Vu et al., 2013), and this has been extended to the recovery and recycling of LIB constituent metals (Meshram et al., 2015; He et al., 2017; Gao et al., 2017; Yue et al., 2018; Verma et al., 2020).

Hydrometallurgical treatment of LIBs

The hydrometallurgical recovery of materials from LIBs chiefly includes pretreatment stages which are preceded by a leaching operation and lastly recovery of the dissolved constituent metals by precipitation or a combination of solvent extraction and precipitation. One could highlight the leaching of the LIB constituents as the main operation in the hydrometallurgical treatment process (Yao et al., 2018). The constituent leaching process directly affects the downstream processing and therefore, if performed optimally could simplify the subsequent separation processes. LIB leaching operations can utilize i) acidic (organic and inorganic), ii) ammoniacal, iii) alkaline or iv) salt solutions (Musariri et al., 2019; Zhang et al., 2018; Chu et al., 2021; Wu et al., 2019; Ku et al., 2016; Zheng et al., 2017; Liang et al., 2021; Dai et al., 2022). Conventional LIB leaching operations apply a combination of acid media and a reducing agent to act as a lixiviant (leaching liquid media) (Pinegar and Smith, 2019; Vishvakarma and Dhawan, 2019). A typical, 7 step, LIB acid-based hydrometallurgical treatment process flow diagram to obtain pregnant leach liquor is given in Fig. 2.

On focusing on the application of inorganic acids, which have proven to be efficient lixiviants in LIB recycling, various configurations have been investigated with results showing that the major acids of choice are sulfuric (H_2SO_4), hydrochloric (HCl) and nitric (HNO_3) acids (Fan et al., 2021; Guimarães et al., 2022; Li et al., 2017; Barik et al., 2017; Xuan et al., 2021; Aaltonen et al., 2017; Aannir et al., 2023). These acidic leaching systems have shown some advantages and disadvantages, which are summarized in Table 2. Examples of reducing agents that have been adopted are hydrogen peroxide (H_2O_2), sodium metabisulphite ($Na_2S_2O_5$) and sodium bisulfite ($NaHSO_3$) (Vishvakarma and Dhawan, 2019; Aannir et al., 2023; Meshram et al., 2016; Vieceli et al., 2018; Tanong et al., 2017). The most common acid/reducing agent lixiviant combination is H_2SO_4/H_2O_2 (Harper et al., 2019; Wang et al., 2016; Gu et al., 2023). The acid/reducing agent chemical synergistic combination is preferred since: i) the acid directly dissolves the metal constituents from the cathode material and ii) the reducing agent lowers the transition metal oxidation states, aiding the dissolution process (Zhao et al., 2020; Zhang et al., 2018).

The conditions used for the major inorganic acid leaching systems are of particular interest and are highlighted in Table 3. The tabulated data shows the use of elevated temperatures in each instance with

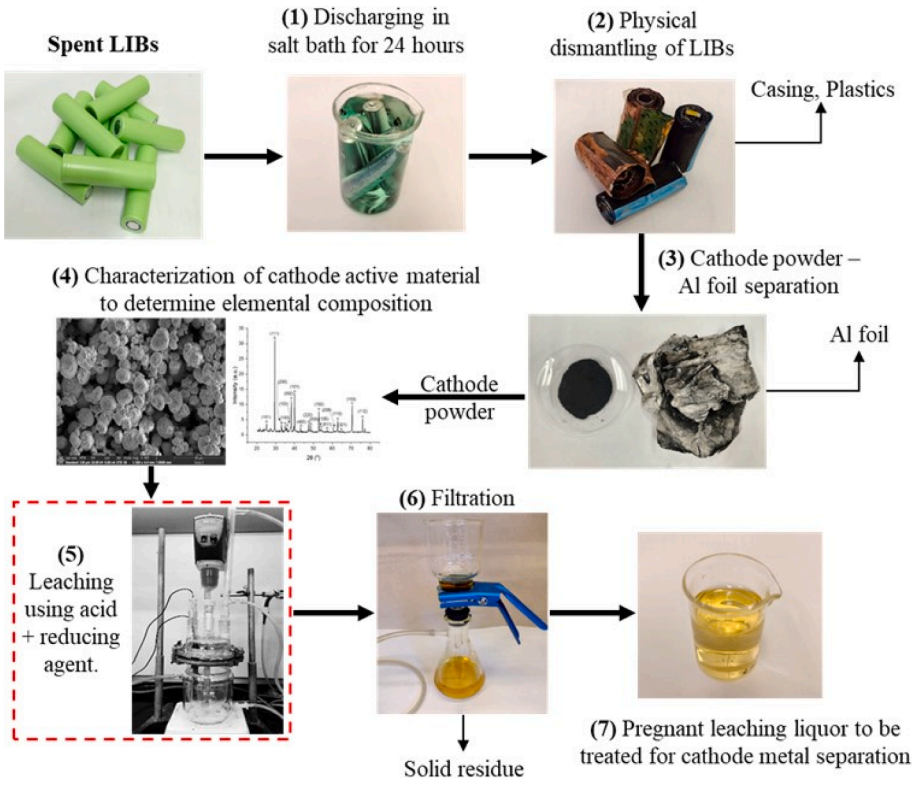

Fig. 2. Process flow diagram for the treatment of LIBs to obtain pregnant leach liquor (adapted and customized from Xu et al. (2008)).

Table 2
Advantages and disadvantages of conventional inorganic acids.

Leaching agent	Advantages	Disadvantages	Ref
H_2SO_4	Direct leaching, fast kinetics, low concentration, high leaching efficiency. Selective leaching for Co(II) and Li(I) over others. Low cost and avoidance of volatility and corrosion problems.	H_2O_2 required to convert some metal ions to more favorable valency states.	(Dutta et al., 2018; Zhu et al., 2012)
HCl	Direct leaching, fast kinetics, high leaching efficiency. Promotes the dissolution of metals because of chloride ions.	High cost, poisonous gas emissions (Cl_2), volatility and corrosion problems.	(Porvali et al., 2019; Guo et al., 2016)
HNO_3	Direct leaching, fast kinetics, low concentration. Selective leaching for Li (I) over others.	Larger amounts of reducing agents required to increase leaching efficiency. Poisonous gas emissions (NO_x).	(Lee and Rhee, 2002; Jung et al., 2021; Lee and Rhee, 2003)

optimal leaching being reported at temperatures between 60–80 ℃ with a reducing agent added to the leaching system. The reducing agent accelerates the leaching kinetics and improves cathode metal recoveries particularly for the transition metals (Zhang et al., 2018; Cerrillo-Gonzalez et al., 2022). However, this translates to a cost associated with i) energy requirements to achieve high temperatures and ii) the use of reducing agents. In addition, these systems result in the evolution of toxic gaseous compounds such as Cl_2, NO_x and SO_3 (Li et al., 2013; Zou et al., 2013; Yao et al., 2015). With these key points, we have focused on investigating the application of alternative acids, particularly the halide group acids, hydrobromic (HBr) and hydroiodic (HI) acid. Both HBr and HI are stronger acids as compared to HCl. The acidity of the hydrogen halides increases in the order: HFl (pKa = 3.14) (Zumdahl and DeCoste, 2012), HCl (pKa = −7.45) (McGrath et al., 2013), HBr (pKa = −9) (Brownstein and Stillman, 1959), HI (pKa = −10) (Brownstein and Stillman, 1959), as the bond strengths of the hydrogen halides determine the relative strengths of the hydrogen halides (Busch, 2018). The larger halides are less charge dense upon solvolysis, causing less solvent order. This is considering the acidity as related to the reaction given by Eq. (1).

$$HA \leftrightarrow H^+ + A^- \quad (1)$$

HI simultaneously acts as an acid and reducing agent (Andrés et al., 1996) and would reduce or potentially eliminate the need for addition of a reducing agent during the leaching process, contributing to energy and cost savings. The use of this conceptual change to leaching is presented in the area highlighted in Fig. 2 (dotted line), which is the focus of this study. We have expanded and explained these details in Fig. 3. The suggested alternative acids are hypothesized to have superior operational considerations, namely, no reducing agent requirement, good kinetic efficiency, which could possibly result in less lixiviant requirements and lower emissions reducing the consequential environmental implications.

This work investigates the application of halide group acids that have to the best of our knowledge not been investigated as potential lixiviants for the recovery of constituent metals during LIB recycling operations. Further, LIB disassembly and recovery of cathode materials from waste LIBs was carried out as a pretreatment stage. A comparison of leaching commercial cathode powder and leaching recovered cathode powder is also provided.

Materials and method

American Chemical Society (ACS) grade HI (55–58 %), HBr (65 %),

Table 3
Conditions used for the various inorganic acid LIB cathode material leaching systems.

Leaching agent	Composition	Conditions		Ref
		Solvent	Recovery	
H_2SO_4	Waste LIB scraps containing Li, CO, Ni, Mn	2 M H_2SO_4, 0.11 M $C_6H_8O_6$ at 80 ℃ for 1.5 h	Li 95.7 %, Co 93.8 %, Cu 0.7 %.	(Peng et al., 2018)
	$LiCoO_2$	2 M H_2SO_4, 5 % H_2O_2 v/v, S/L 10 % w/v at 75 ℃ for 1 hr.	Li 99.1 %, Co 70 %	(Jha et al., 2013)
	Mixed cathode materials containing Li, Co, Ni, Mn	1 M H_2SO_4, S/L 5 % w/v at 95 ℃ for 4 h	Li 93.1 %, Co 66.2 %, Ni 96.3 %, Mn 50.2 %	(Meshram et al., 2015)
	Reduced $LiCoO_2$	2.25 M H_2SO_4, S/L 10 % w/v at 80 ℃ for 0.5 h	Li ~ 100 %, Co ~ 100 %	(Yue et al., 2018)
HCl	$LiCoO_2$	4 M HCl at 80 ℃ for 2 h	Li 97 %, Co 99 %	(Li et al., 2009)
	$LiCoO_2$ + $LiMn_2O_4$ + $LiNi_{1/3}Co_{1/3}Mn_{1/3}O_2$	4 M HCl, S/L 5 % w/v at 80 ℃ for 1 hr.	Li, Ni, Co, Mn > 99 %	(Wang et al., 2009)
	$LiCoO_2$	3 M HCl, 3.5 % H_2O_2 v/v, S/L 5 % w/v at 80 ℃ for 1 hr.	Li, Co 89 %	(Shuva and Kurny, 2013)
HNO_3	$LiCoO_2$	1 M HNO_3, 1.7 % H_2O_2 v/v, S/L 1–2 % w/v at 75 ℃ for 0.5 h	Li, Co > 95 %	(Lee and Rhee, 2003)
	Mixed cathode materials containing Li, Mn	2 M HNO_3 at 80 ℃ for 2 h	Li ~ 100 %	(Castillo et al., 2002)

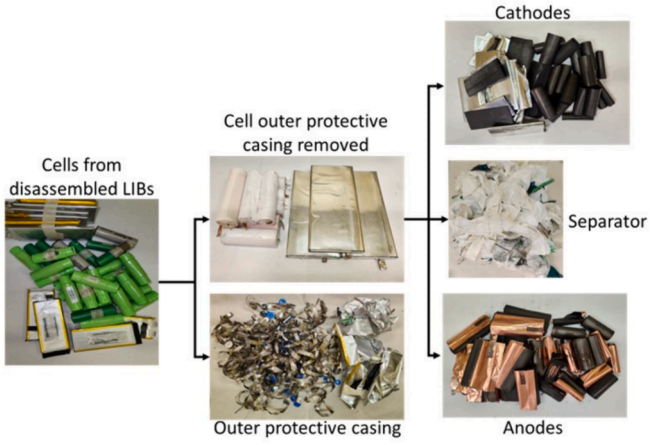

Fig. 3. The a) conventional acid leaching process and b) our proposed acid leaching process for LIBs. Note the differences between a) and b) are not only the type of acids used for leaching but also the presence and absence of reducing agent(s) in a) and b) respectively.

HNO_3 (70 %), HCl (37 %) and NaCl (>99 %) were purchased from Thomas Scientific. Cathode material ($LiNiCoMnO_2$ [Ni:Co:Mn = 5:2:3]) in powder form was purchased from MTI Corporation. Spent LIBs were obtained from a local waste management facility. All solutions were freshly prepared using deionized water (resistivity ≥ 18 MΩ.cm at 25 °C) obtained from a Millipore Direct-Q® 3 UV Water Purification System. Collected samples were analyzed by inductively coupled plasma mass spectroscopy (ICP-MS) using a Shimadzu 2030 inductively coupled plasma mass spectroscope. A Beckman-Coulter LS 13 320 particle size analyzer was used for powder particle size analysis. Scanning electron microscopy (SEM) and energy dispersive X-ray spectroscopy (EDXS) were conducted using a Thermo Scientific™ Scios™ 2 FIB-SEM. A Bruker D8 ADVANCE X-ray diffractometer (Cu Kα radiation, 40 mA, 40 kV) was used for X-ray crystallography. Thermal analysis was conducted using TA Instruments' TGA Q500 with platinum (Pt) pans.

Cathode material recovery

The collected LIBs, which were made up of cylindrical and pouch cells, were initially pretreated through discharging and disassembly before the cathode material was recovered. The cells were disassembled in a manner to maintain the integrity of the different components, minimizing cathode powder contamination. To safely conduct cell disassembly, the LIB cells initially required discharging to a safe state of charge (SOC) to prevent short-circuiting (Tembo et al., 2024). Aqueous discharging using a 10 wt% NaCl solution was utilized as it is easy to implement and control. To prevent corrosion of the LIB cells by Cl^- ions, the cells were discharged ex-situ by connecting the cell leads (via Cu wires) to sacrificial Fe electrodes which were immersed in the prepared NaCl solution. The cell voltages were tracked over a 24-hour period, until they were under 2 V, which was ascertained as a safe voltage for cell disassembly.

A scalpel was used to manually cut open the pouch cells' outer covering to expose the rolled electrode assembly. Disassembly of the cylindrical cells was initiated at the cell cathode end, wherein the cylindrical cells were unsealed at the seam followed by unrolling the steel casing from the rolled-up electrode assembly. Subsequently, the anodes, cathodes and separators were then recovered separately after unrolling the rolled electrode assemblies. Thermal treatment was used to recover the cathode powder from the aluminum (Al) foils. Thermogravimetric analysis (TGA) was conducted on the cathode foils to determine the appropriate temperature for binder decomposition which would enable the recovery of the cathode powder from the Al foils. The temperature was raised at 10 ℃/min from 25 to 600 °C under a constant air flow rate of 60 ml/min. Upon determination of the appropriate operating temperature to enable cathode powder recovery, the cathode foils were thermally treated in a muffle furnace for 30 min at 580 ℃ after which, the cathode powder was lightly scrapped off the Al foils and collected for further treatment.

Leaching experiments

Initial leaching experiments to determine proposed acid performance were performed in flat bottomed flasks utilizing commercial cathode material, with heating accomplished using heating plates with stirring capabilities. The stirring was achieved by use of magnetic stirrers at 200 rpm. Upon establishing the performance of the proposed lixiviants on utilizing commercial cathode materials, subsequent experiments were conducted to determine the effective leaching conditions for leaching metals from spent cathode material. A jacketed reactor with an overhead stirrer assembly operating at 300 rpm with installed pH and temperature probes was utilized for the spent cathode material experiments.

Determination of lixiviant concentration

Three different concentrations were selected for each acid: 1, 2 and 3 M for HBr and 1, 1.5 and 2 M for HI. These concentrations were selected based on the relative strength of each acid in comparison to conventionally utilized acids. With a high pKa value, the selected HI concentration range was narrower, while that of HBr was relatively broader than that of HI but lower than that of the conventionally used inorganic acids. The lowest S/L ratio that would be investigated (30 g/L) was used for the optimum concentration determination while system temperature

was maintained at the highest temperature of 80 ℃ that would be considered during this study.

Determination of optimum solid to liquid ratio

The solid to liquid (S/L) ratio is the mass of solids that come in contact with a given volume of lixiviant. The S/L ratio has a significant impact on the leaching operation as this determines the amount of lixiviant that is available to optimally leach the desired metal. Since the leaching operation is a mass transfer process, it heavily depends on the availability of lixiviant to effectively carry the leached-out component. Different cathode material masses were added to a fixed volume of lixiviant (100 mls) to give the different S/L ratios. The investigated S/L ratio range was 30–60 g/L. Previously established acid concentrations were used, while the temperature was maintained at 80 ℃ for each of the optimum S/L ratio determination experiments. Each experimental run was conducted for an hour.

Determination of temperature effects

Temperature greatly influences the leaching kinetics and overall metal recoveries. The cathode material was subjected to leaching within the temperature ranging from 40 to 80 ℃, at the optimum established lixiviant concentrations and S/L ratios to investigate the kinetics of the leaching process. Solution samples were collected at various intervals for a total of 2 h.

Results and discussion

Cell disassembly and cathode powder recovery

Each cell was discharged to under 2 V after which any plastic wrappings were removed, and each cell was disassembled as described earlier. The product flow diagram realized during the cell disassembly process, leading to cathode recovery, is given in Fig. 4.

On recovering the cathode foils, TGA was utilized as a means of determining the temperature for effective decomposition of the cathode binder thereby allowing for cathode powder recovery. Samples of recovered cathode foils from the spent LIB cells were initially analyzed. The TGA results are given in Fig. 5. Changes in the sample weights were pronounced for the cathode foils relative to the cathode powders. It has been reported that binder decomposition typically begins at 350 ℃ (Hanisch et al., 2015). From Fig. 5 the visible onset temperature for marked decomposition can be highlighted at 220 ℃ for the pouch cell cathode foils and 310 ℃ for the cylindrical cell cathode foils. It has been determined that a decrease in the onset temperature for binder decomposition may be attributed to binder exposure to the electrolyte organics which may consist of mixtures of diethyl carbonate, dimethyl carbonate, ethylene carbonate, possibly affecting the binder and the binder-Al foil adhesion (Chen et al., 2013).

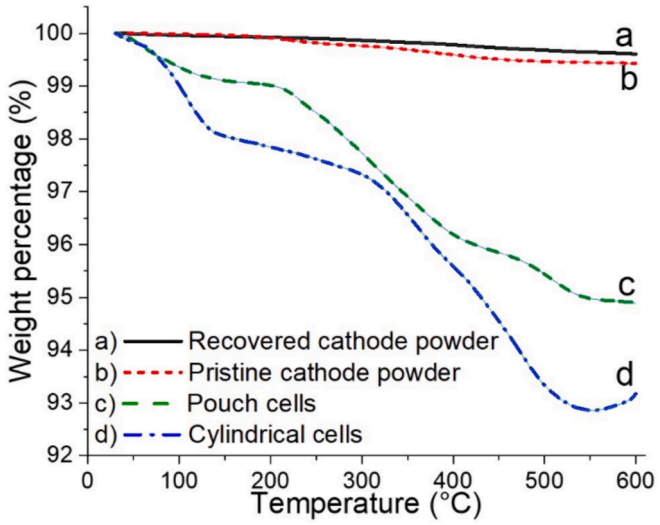

Fig. 4. Li-ion cell disassembly process.

Upon onset of the binder decomposition, both pouch and cylindrical cells show a sharp loss in weight owing to volatilization of the binder. The pouch cell foils showed a reduction in mass loss at 400 ℃ and similarly, the cylindrical cell foils experienced a reduction in mass loss at 400 ℃. Pouch cell cathode foils exhibited an increase in mass loss at 470 ℃ while that of the cylindrical cells remained constant up to 550 ℃. Weight decrease of both foils ceased above 560 ℃, which can be taken as the end point for the binder decomposition. The temperature was further raised to 600 ℃ and kept constant, which did not result in further cathode foil weight loss. It was therefore determined that based on literature and current TGA results from the studied samples, thermal treatment to recover the cathode powder from the Al foils would be conducted at 580 ℃ for a 30-minute period. On thermal treatment of the recovered LIB cathode foils, cathode powder was recovered from the Al foils, subjected to TGA treatment, and compared with pristine, commercially sourced LIB cathode powder. The pristine and recovered cathode powders exhibited somewhat similar trends, retaining most of their mass throughout the TGA testing. A slight difference was observed between the two cathode powders which was attributed to the recovered cathode powder initially undergoing thermal treatment during the recovery process.

Characterization

The different sample morphologies were analyzed using SEM operated in secondary electron mode. The recovered cylindrical and pouch cell cathode foil images are given in Fig. S1 and clearly show the disintegrated structure of the cathode layer with presence of artifacts which can be attributed to exposure to the electrolyte. The cathode material grain sizes and orientations are irregular, as shown in Fig. S2, which can be due to the repeated cycling of the LIB cells ultimately affecting the morphology. SEM images of the recovered LIB cathode powder and pristine LIB cathode material were compared in Fig. 6. Pristine cathode material SEM images showed particles of regular spherical shapes while the recovered cathode powder particles were irregularly shaped. Furthermore, the surface characteristics differed between the different cathode powders. The pristine cathode powder particle images showed a rough particle surface while the recovered cathode powder images pointed to a smoother particle surface with signs of contour presence.

EDXS was performed on both the recovered and pristine cathode powders. The pristine cathode powder EDXS mapping results given in Fig. S3 show a uniform distribution of the metals Co, Mn and Ni in the cathode powder. While the EDXS mapping of the recovered cathode powder given in Fig. S4 shows a less uniform distribution of the cathode metals. X-ray diffraction (XRD) performed on the cathode powder samples provided the results shown in Fig. 7 which indicates that the powders conformed well to the NMC LIB chemistry, as referenced using the crystallography open database (COD). The metal content in the pristine and recovered cathode powders was determined by aqua regia ($HCl:HNO_3$ molar ratio of 3:1) digestion of the cathode powders and the results are given in Table S1. Particle size analysis was conducted on the pristine and recovered cathode powders and the particle size distributions are given in Fig. 8. The pristine cathode powder had a narrower size distribution with a mean particle size of 12.5 μm and 90 % of the powder had a particle size of less than 18.5 μm. The recovered cathode powder had a broader size distribution as evidenced by a mean particle size of 17.3 μm while 90 % of the powder had a particle size less than 30.4 μm.

Owing to these differences in the morphological structure and particle size of the cathode powders, it was determined that while pristine cathode powder could be leached, the leaching mechanisms and kinetics could be different from those of the recovered spent LIB cathode powder.

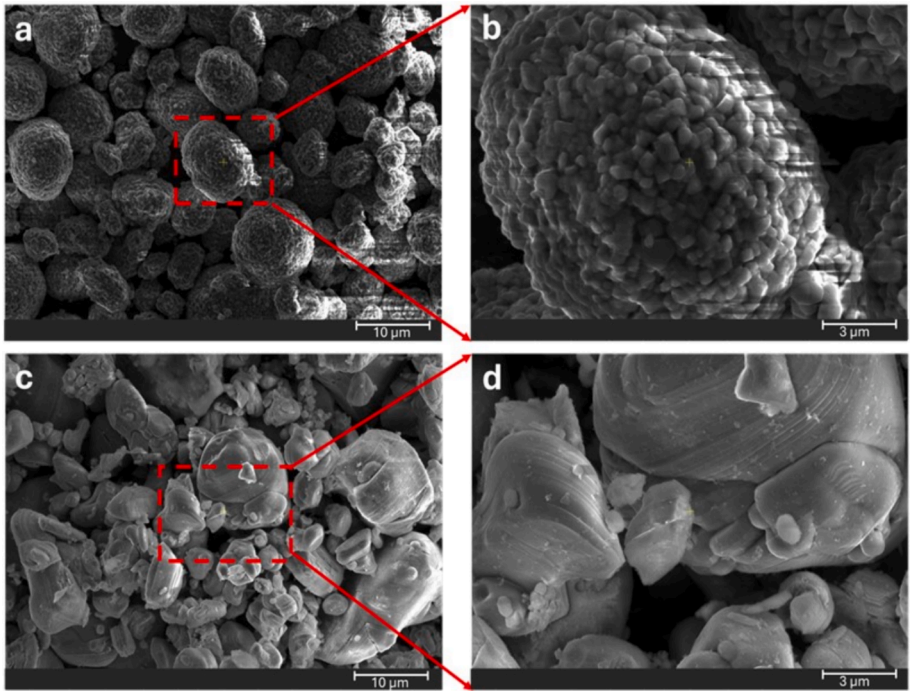

Fig. 5. TGA results of recovered cathode foils from spent LIBs, pristine and recovered LIB spent cathode powder.

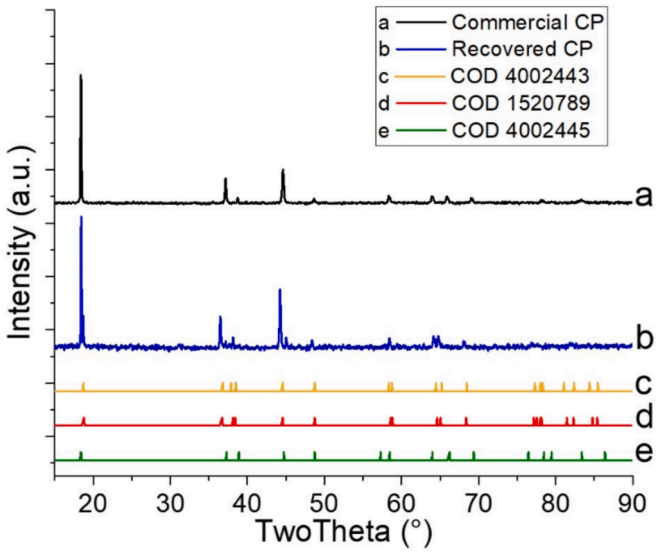

Fig. 6. a)-b) Pristine and c)-d) recovered LIB cathode powder SEM SE images.

A study was therefore performed on both the pristine commercial cathode powder and on the recovered LIB cathode powder.

Commercial cathode powder leaching

To establish the performance of the chosen lixiviants for LIB cathode material leaching, commercial cathode powder was initially used for the leaching process. Metal recoveries were evaluated for each lixiviant system utilizing the conditions given in Table 4. The system operating conditions were independently evaluated for the commercial powder and the recoveries obtained for the different metals under the conditions given in Table 4 are given in Fig. 9. It can be noted that the lixiviants achieve good metal recoveries from the commercial cathode material with Li recovery being the highest in the given time frame. Owing to the rapid rate of leaching of the cathode powder, EDXS was performed on commercial cathode powder that had been leached for 10 min and the mapping is shown in Figs. S5 and S6 for the HBr and HI system respectively. The EDXS mapping results show more rapid leaching of the metals in the HI system compared to the HBr system. The results from the initial leaching tests utilizing the commercial cathode material proved that the lixiviant systems could effectively be used for leaching of the metals from LIB cathode powder and so the question that needed to be answered next was, how would these systems perform in the case of leaching metals from cathode material recovered from spent LIB cells.

Recovered cathode powder leaching

Determination of lixiviant concentrations

Investigations related to the operating lixiviant concentrations for the lixiviant systems were conducted utilizing a fixed S/L of 30 g/L and a temperature of 80 °C. 30 g/L was selected as an average S/L based on the HCl lixiviant system whereas 80 °C was selected as this was the maximum operating temperature selected for this study. The results given in Fig. 10, showed an increase in the metal recoveries with an increase in the lixiviant concentration. The effect of concentration on the metal recoveries can be explained by considering Fick's law of diffusion, which quantitatively explains the diffusion rat (Seliverstov, 2016) and in its simplest form is given by Eq. (2) (Griskey, 2005).

$$J = -D\frac{dC}{dx} \tag{2}$$

In Eq. (2), J is the diffusion flux, D is the diffusion coefficient (diffusivity), C is the volume concentration of the diffusing component in the x direction and dC/dx gives the concentration gradient. Therefore, the diffusion of species depends on the concentration gradient with the diffusion direction of the diffusing component being in the opposite direction to the concentration gradient (Fan et al., 2020). Considering a spherical solid particle from which the component is leaching from, the concentration of acid influences the ion diffusion velocity and the concentration of proton (H^+). As the lixiviant concentration increases in the leaching system, so does the concentration of H^+ present. This results in a large difference in concentration between the solid–liquid interphase,

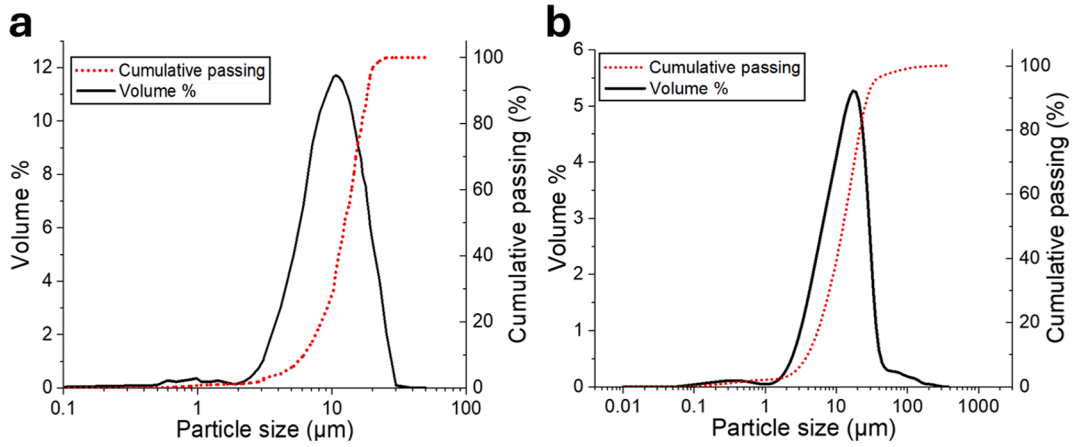

Fig. 7. XRD patterns of the pristine commercial and recovered cathode powder (CP) with highlighted crystallography open database (COD) reference LIB chemistries.

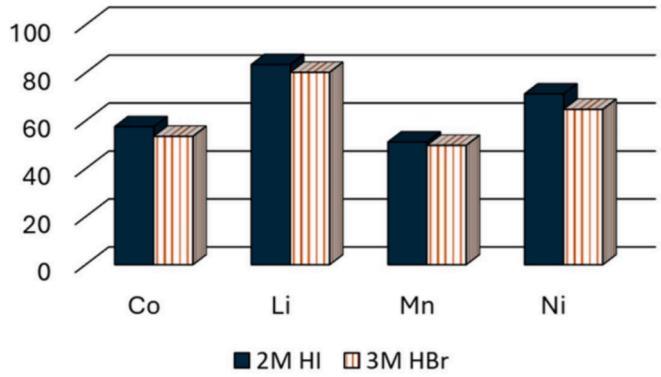

Fig. 8. Particle size distribution for a) pristine and b) recovered LIB cathode powder.

Table 4
Summary of conditions utilized for metal leaching from the HBr and HI systems.

System	Concentration (M)	S/L ratio (g/L)	Temperature (℃)	Time (mins)
HI	2	12	60	30
HBr	3	9	60	30

where the reaction occurs, and the bulk of the solution which in turn increases the diffusion rate. This explains the trend seen, wherein an increase in acid concentration increases the metal leaching efficiency and consequently, the metal recovery. The optimum metal leaching for the four metals under investigation was achieved at concentrations of 2 M HBr and 1.5 M HI. Although in the case of HBr, maximum recoveries were achieved using the 3 M HBr, the differences in the recoveries owing to the change in the acid concentrations would not warrant the use of the higher acid concentration. As such concentrations of 2 M HBr and 1.5 M HI were selected for the preceding investigations.

Optimum solid to liquid ratios

The S/L ratio experiments resulted in the establishment of an optimum leaching S/L ratio for each lixiviant system. Fig. 11 shows the results from the HBr (a–d) and HI (e–h) S/L ratio determination experiments. In each instance the metal recoveries steadily increased with an increase in the S/L ratio until a maximum metal recovery was achieved. This increase in metals recovery is to be expected as more metal is accessible for leaching per given volume of lixiviant. After the optimum metal recovery point, the metal recoveries dropped with an increasing S/L ratio. The most likely reason for the decrease in recoveries on increasing the S/L ratio past the optimum could be attributed to mass transfer resistance and solid–liquid contact. Literature suggests that an increase in the S/L ratio past the optimum increases the mass transfer resistance at the solid/liquid interface which in turn affects the metal recoveries (Sitando and Crouse, 2012). The concentration gradient existing at the interface boundary builds up and slows down the constituent leaching kinetics from the bulk of the material which results in less recoveries than optimum for the given leaching period. An increase in the S/L ratio also decreases the amount of lixiviant present to react with the cathode material per unit mass of cathode material (Zheng et al., 2017; Nayl et al., 2017). Taking into consideration the leaching efficiencies, preceding leaching experiments were carried out at the optimum S/L ratios of 40 g/L for the HBr and HI systems.

Effect of leaching temperature

After establishing the optimum concentration and S/L ratios for each system, the metal recovery studies were conducted at a temperature range of 40–80 ℃. Fig. 12 a)–d) and e)–h) show the metal recovery results that were obtained in the HBr and HI systems respectively for each metal. The initial 40 min of contact time showed the highest leaching rate in both systems, and the highest metal recoveries were achieved at 80 ℃ for the HBr system and 60 ℃ for the HI system. The highest recoveries of the constituent metals, Co, Li, Mn and Ni in the HI system were 92.9 %, 93.6 %, 93.1 % and 94.5 % respectively, at an operating temperature of 60 ℃ and with a 1.5 M HI concentration. The HBr system achieved metal recoveries of 93.8 %, 92.0 %, 83.7 % and 99.7 % for Co, Li, Mn and Ni respectively, at 80 ℃ and using 2 M HBr. Even though the HBr system achieved the highest recoveries at 80 ℃, the metal recoveries in the 60–80 ℃ temperature range were comparative, such that, lower operating temperature could be used to achieve good metal recoveries. Therefore, a temperature of 60 ℃ was selected for optimal operation in the HBr system, wherein the achieved metal recoveries on using a 2 M HBr solution were 90.6 %, 89.1 %, 83.1 % and 96.4 % for Co, Li, Mn and Ni respectively. EDXS mapping and XRD were conducted on the recovered cathode powder after leaching for 10 min and the results are given in Figs. S7, S8 and S9. It can be noted that the leached recovered cathode powder EDXS mapping shows a similar trend as that of the leached commercial cathode powder, wherein, the rate of metal leaching is faster in the HI system than the HBr system. The XRD patterns clearly show a reduction in peak intensities with leaching and a disappearance of some of the peaks, as compared to that of the recovered cathode powder pre-leaching.

The proposed cathode material leaching reaction in a hydrohalic acid medium can be expressed by Eq. (3) (Xuan et al., 2019).

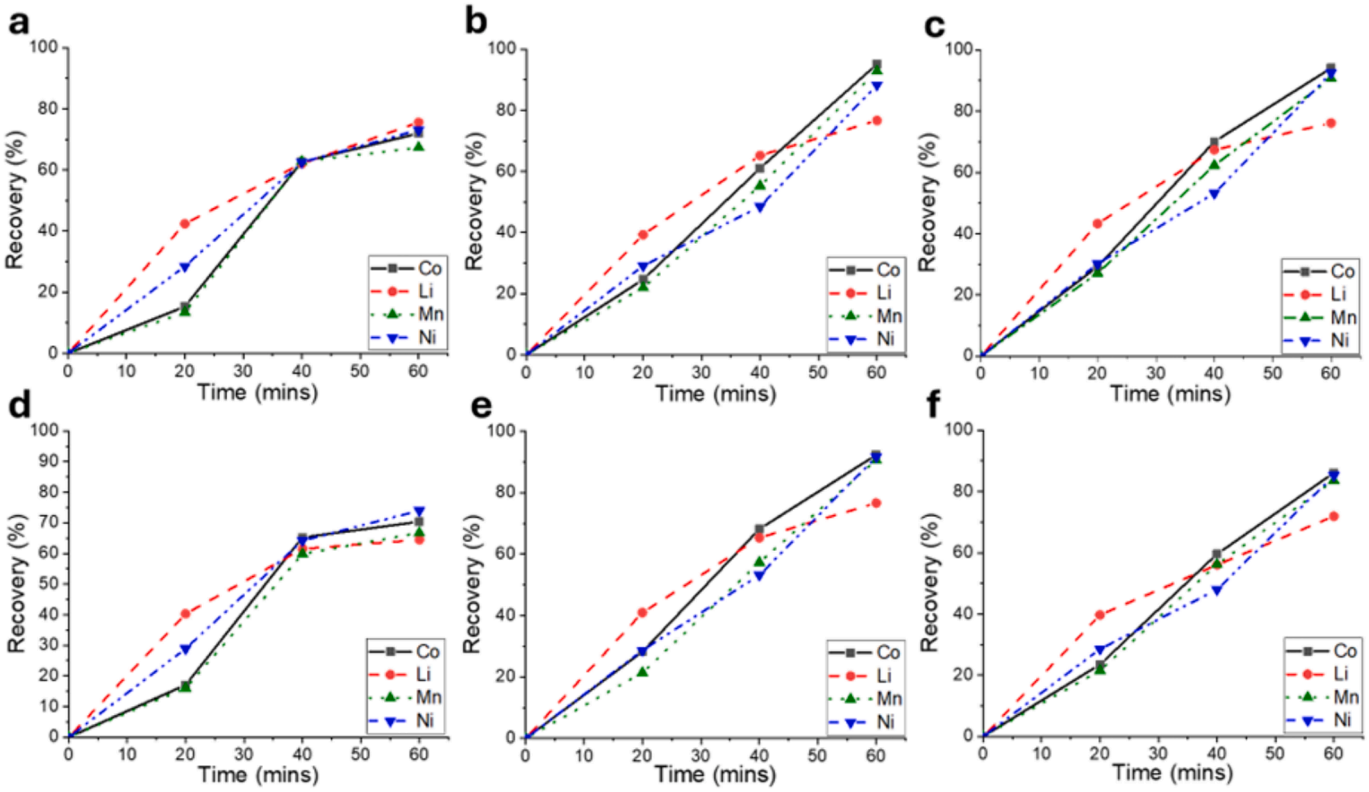

Fig. 9. Metal recoveries for the HBr and HI leaching systems using commercial LIB cathode powder.

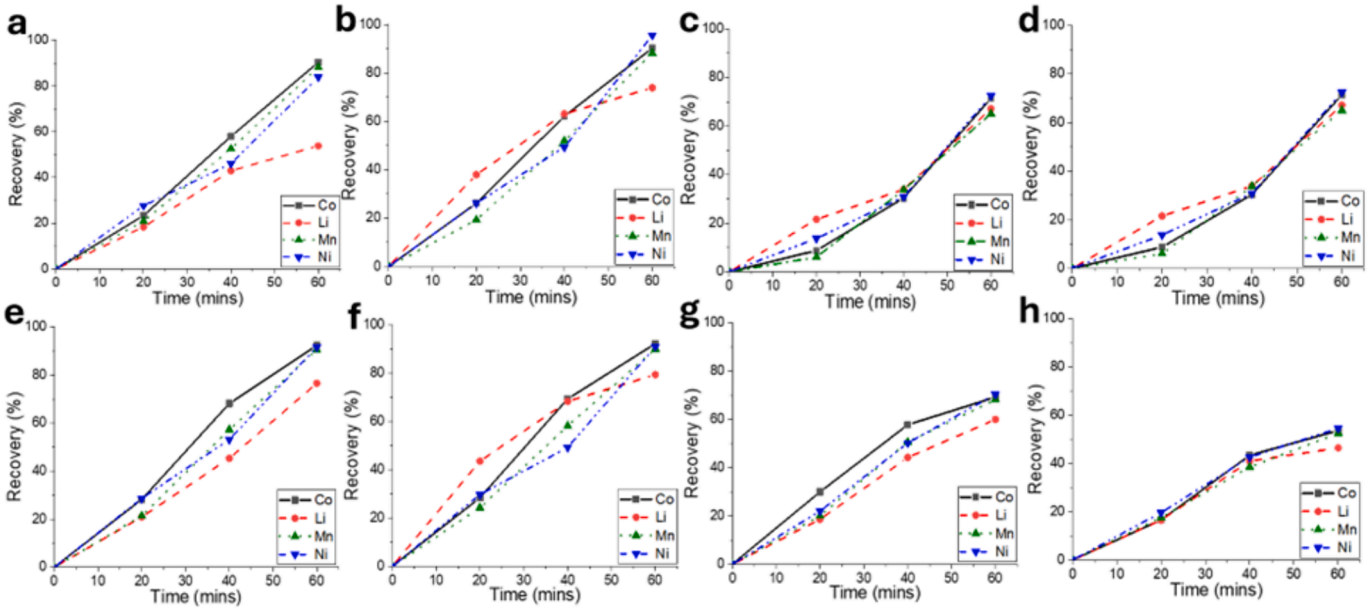

Fig. 10. Co, Li, Mn and Ni recoveries as a function of time for a)1 M HBr, b) 2 M HBr, c) 3 M HBr, d) 1 M HI, e) 1.5 M HI and f) 2 M HI at 30 g/L S/L ratio and 80 ℃.

$$2LiMO_{2(s)} + 8HAc_{(aq)} \leftrightarrow 2LiAc_{(aq)} + 2MAc_{2(aq)} + 4H_2O_{(l)} + Ac_{2(g)} \quad (3)$$

for Ac = Br, I and M = Ni, Mn and Co. Brown Br_2 and violet I_2 vapors were observed during the experiment. Clear capture of the halide vapors was observed in the clear glass condenser as the color gradient within the condenser went from the characteristic vapor color to clear up along the condenser length. In the case of iodine, dark crystals, characteristic of solid iodine, developed at the condenser surface closest to the vessel, as seen in Fig. S10. The general trend observed from the leaching data was an increase in the percent metal recoveries with an increase in the operating temperatures.

As the temperature increases so does the reaction rate constant meaning that there is an increased propensity for the reaction to proceed to form the products. The rate constant can be a function of parameters such as ionic strength, however, it is strongly dependent on temperature such that the general assumption that the rate constant only depends on temperature holds very well (Westmoreland, 1993). As such, the increase in temperature increases the rate kinetics which in this case

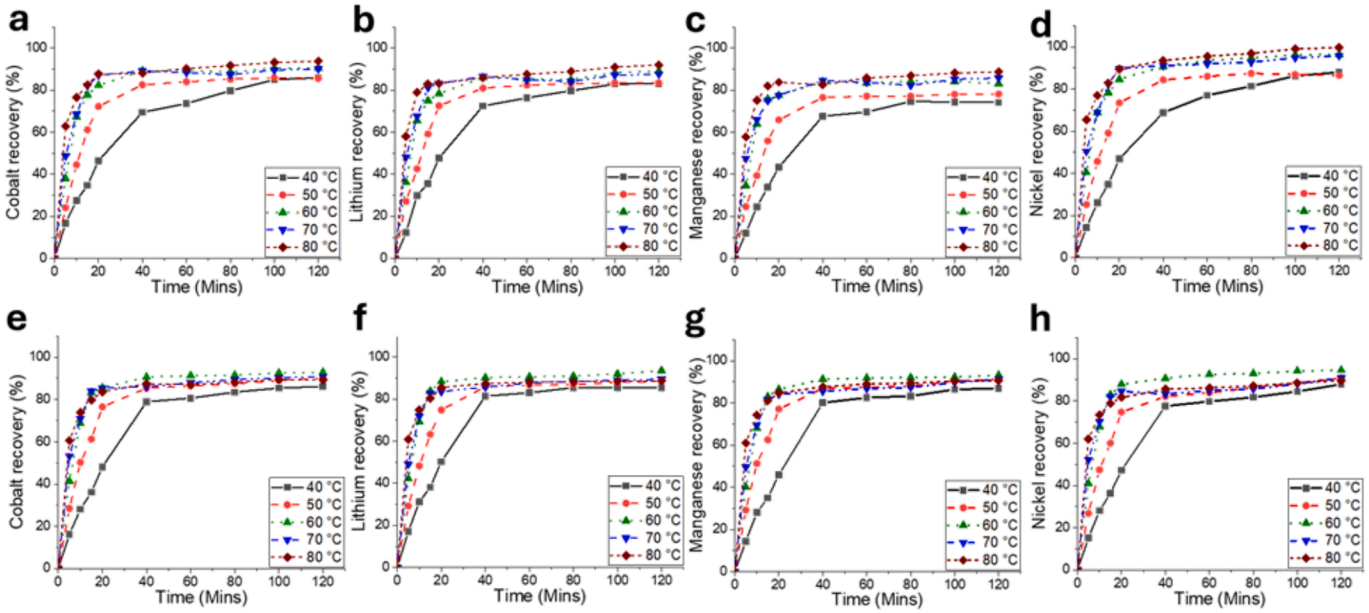

Fig. 11. Varying S/L ratios of a) 30 g/L, b) 40 g/L, c) 50 g/L, d) 60 g/L for he HBr system and e) 30 g/L, f) 40 g/L, g) 50 g/L and h) 60 g/L for the HI system.

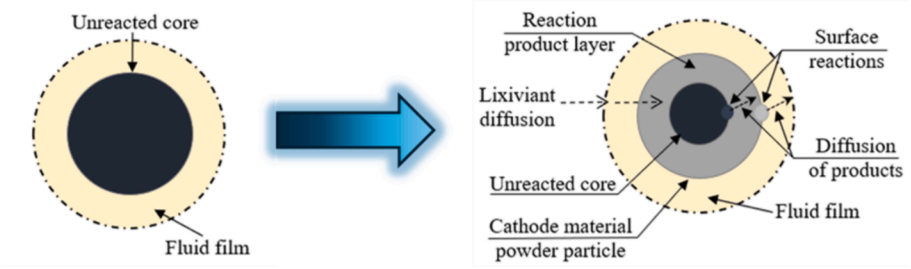

Fig. 12. a)–d) HBr system metal recoveries and e)–h) for the HI system.

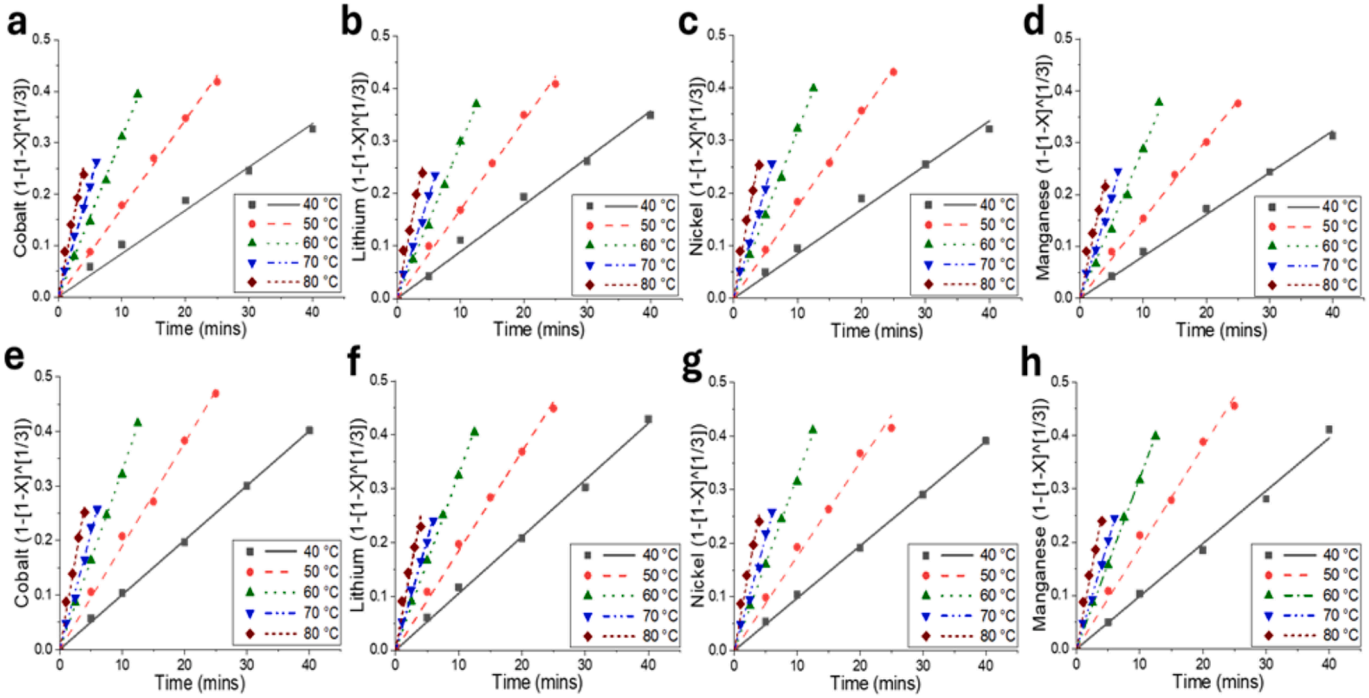

Fig. 13. Shrinking core model pictorial depiction.

results in greater metal recoveries at higher temperatures for the same lixiviant concentrations. On a micro level, an increase in temperature increases the motion of molecules present in the system which in turn promotes the reaction (Fan et al., 2020). This increased molecule motion contributes to bond distortion and stretching which contributes to bond breakage and new bond formation.

Kinetics

Kinetic analysis can offer mechanistic insights into the extraction process. To this end, an attempt to elucidate the kinetics associated with LIB cathode powder leaching by HBr and HI using the leaching results obtained at the various temperatures, ranging from 40 ℃ to 80 ℃, was systematically conducted. The shrinking core model, which has been applied to numerous investigations (Peng et al., 2018; Jha et al., 2013; Xing et al., 2021; Lin et al., 2021; Zheng et al., 2018) involving LIB leaching studies from LIB materials, was utilized. A pictorial depiction of the shrinking core model steps when treating an unreacted core is given in Fig. 13. The shrinking core model divides the leaching reaction into the following steps: i) diffusion of lixiviant through the fluid–solid interface; ii) diffusion of lixiviant molecules to the unreacted core surface through the fluid–solid interface and adsorption of the lixiviant molecules by unreacted solid; iii) reaction of adsorbed lixiviant molecules with unreacted solid and product release; iv) diffusion of reaction product to the solid–fluid interface through the reaction product ash layer; v) diffusion of reaction product into the fluid (Setiawan et al., 2019). Furthermore, according to the shrinking core model, the reaction product may completely, partially or not dissolve in the fluid, which gives rise to models describing a shrinking particle, shrinking core (constant particle size) and shrinking core (shrinking particle).

Elucidation on the rate-determining step was conducted using models defining the earlier highlighted scenarios describing the dissolution of a crystal structure considering ash layer diffusion (boundary layer) control (Eqs. (4), (5) and (6)), chemical reaction (chemical reaction at partial surface) control (Eq. (7), parabolic product layer diffusion control (Eq. (8)), Stoke's regime (Eq. (9)) and crystal dissolution (Eq. (10)) (Xuan et al., 2021; Dickinson and Heal, 1999). Furthermore, the function of the recovery [f(X)] can be related to the particle size through Eq. (11). (Xuan et al., 2021)

$$kt = 1 - 2X/3 - (1 - X)^{2/3} \tag{4}$$

$$\mathrm{k}\ln t = \left[1 - (1 - X)^{1/3}\right]^2 \tag{5}$$

$$kt = 1 - 3(1 - X)^{2/3} + 2(1 - X) \tag{6}$$

$$kt = 1 - (1 - X)^{1/3} \tag{7}$$

$$kt = X^2 \tag{8}$$

$$kt = 1 - (1 - X)^{2/3} \tag{9}$$

$$kt = [-\ln(1 - X)]^{2/3} \tag{10}$$

$$f(X) = kt = 3\beta[HAc]/\rho_S R_o \tag{11}$$

In the above equations, k is specific rate of reaction or rate constant, t is the time, X is the fractional recovery, β is the mass transfer coefficient, [HAc] is the acid concentration, ρ_s is the solid density and R_o is the initial particle (core) radius. The experimental data was fitted into each of the above highlighted model equations (after linearization) to ascertain which model best described the metal leaching kinetics for each lixiviant. The initial data fit for each acid was performed using the recoveries at varying temperatures and the leaching conditions (acid concentration and S/L ratio) identified as the most ideal for each acid. Using the recovery data from leaching at different temperatures between 40–80 ℃, a S/L ratio of 40 g/L and concentrations of 2 M HBr and 1.5 HI, kinetic plots were generated. The data fit Eq. (7), and the resulting plots that were generated are given in Fig. 14. Applying statistical regression, the HBr (Fig. 14a–d) and HI (Fig. 14e–h) systems indicate a good data fit since the value of the coefficient of determination (R^2) is close to 1 (>0.99) for the data fitted into the kinetic equation. This R^2 value indicates that most of the variability in the response variable is explained by the fitted model. Based on the obtained kinetic data, metal leaching for both systems can be surmised to be chemical reaction controlled. Using the Arrhenius equation (Eq. (12)) where k denotes the rate constant, A is the pre-exponential factor, E_a is the activation energy, R is the ideal gas constant and T is the temperature, the activation energies for leaching of the metals in the leaching systems can be determined.

$$k = A \times e^{-E_a/RT} \tag{12}$$

$$\ln k = \ln A - E_a/R \; {}^{1}/_{T} \tag{13}$$

Re-arranging Arrhenius' equation to obtain a linear form (Eq. (13)), the activation energies for the HBr and HI systems were determined by plotting ln (k) as a function of T^{-1} in Fig. 15. The activation energies were determined as for each metal in the HBr and HI leaching system and are reported in Table 5. The apparent activation energy associated with metal leaching in the HBr system was greater by an average of 8.9 % than that of the HI system. A greater activation energy translates to a higher energy barrier to be overcome by the reaction, meaning that it is more difficult for it to proceed (Xu et al., 2021). This explains the metal recovery differences between the HBr and HI systems. The calculated activation energies agreed well with the ascertained chemical reaction controlled model (shrinking particle) as typically, the activation energy for a diffusion controlled process is less than 40 kJ/mol while the activation energy for a chemical reaction controlled process is typically greater than 40 kJ/mol (Espiari et al., 2006). The particle size influences the leaching recovery as it directly determines the surface area available for solid–liquid interaction. Furthermore, the initial particle size directly contributes to the process kinetics as highlighted by Eq. (11). This, along with the metal concentration gradient, explains the initial rapid leaching of the metals.

The presented results show that HBr and HI can successfully be utilized in leaching metals from LIB cathode powders, however, consideration of the environmental and economic implications of their utilization needs to be addressed. Like other inorganic acids, utilization of HBr and HI requires adequate waste handling to prevent negative environmental impacts (Sigma-Aldrich, 2024a,b). The environmental implications of utilizing the proposed acid systems may be evaluated using a life cycle assessment study (Tembo et al., 2024). Given the presented leaching systems, an effective way of managing HBr and HI environmental impacts would be the recovery and recycling of the acids. A key area of consideration is post-leaching treatment, with solvent extraction being proven to be a viable option for recovering acids for recycling (Tembo et al., 2024; Tang et al., 2023; Vieceli et al., 2023). Furthermore, use of solvent extraction would reduce the economic cost associated with using the proposed hydrohalic acids which can have a cost of an upwards of 7 times that of conventional inorganic acids utilized (Chemanalyst, Hydrobromic Acid Price Trend and Forecast, 2024a, b).

Conclusions

This work provides a detailed analysis into the recovery of Co, Li, Mn and Ni (LIB cathode material metals) from LIBs, by application of the hydrohalic acids, HBr and HI as novel lixiviants. Initial pretreatment of collected waste LIBs, involving the discharging and disassembly of the

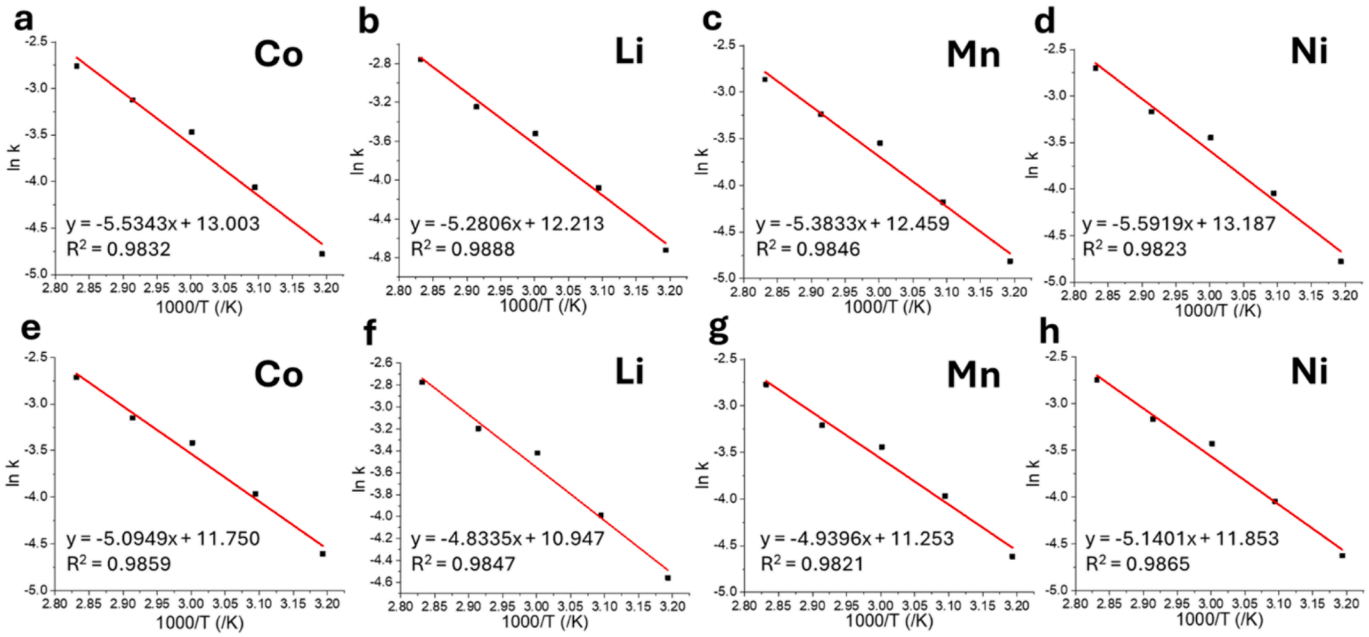

Fig. 14. Kinetic data fit for the a)–d) HBr system and e)–h) the HI system corresponding to the respective model equation.

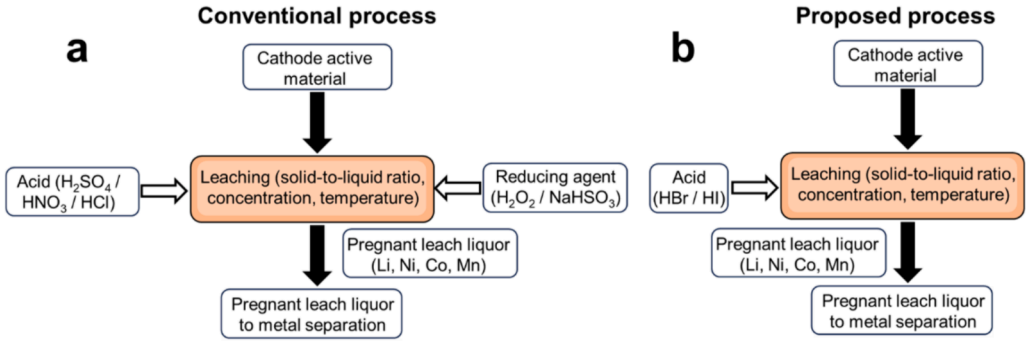

Fig. 15. ln k vs 1/T data fit for a) Co, b) Li, c) Mn, d) Ni for the HBr system and e) Co, f) Li, g) Mn and h) Ni for the Hi system.

Table 5
Activation energies for leaching of the different metals in HBr and HI system.

	Activation energy (kJ/mol)			
System	Co	Li	Mn	Ni
HBr	46.01	43.90	44.76	46.49
HI	42.36	40.19	41.07	42.73

LIB cells, is presented. Studies into the recovery of cathode powder from the Al foil established a temperature of >560 ℃ for successful recovery of the cathode powder. A probe into the morphology of cathode foils, recovered cathode powder and pristine commercial cathode powder highlighted structural differences believed to have an impact on relating data from studies utilizing pristine cathode material versus studies utilizing recovered cathode material. A systematic leaching study was performed to determine the optimum lixiviant concentrations, solid to liquid (S/L) ratios and operating temperatures. Optimum recoveries of the constituent metals, Co, Li, Mn and Ni from the recovered cathode powder in the HI system were 92.9 %, 93.6 %, 93.1 % and 94.5 % respectively, at an operating temperature of 60 ℃, S/L ratio of 40 g/L and a 1.5 M HI concentration. The HBr system achieved metal recoveries of 90.6 %, 89.1 %, 83.1 % and 96.4 % for Co, Li, Mn and Ni respectively, at 60 ℃, a S/L ratio of 40 g/L and using 2 M HBr. Kinetic studies showed that the constituent metal dissolution process is chemical reaction controlled in both the HBr and HI systems. On establishing the appropriate models, the different values of the diffusion rate constant (k) associated with the specific leaching process were then calculated. The Arrhenius equation was used to evaluate the activation energies for Co, Li, Mn, and Ni which were determined as 46.01 kJ/mol, 43.90 kJ/mol, 44.76 kJ/mol and 46.49 kJ/mol for the HBr system and 42.36 kJ/mol, 40.19 kJ/mol, 41.07 kJ/mol and 42.73 kJ/mol for the HI systems respectively. This work points to the applicability of the previously unexplored halide-based acids, HBr and HI in the absence of a reducing agent in recovering constituent metals from LIB cathode materials.

CRediT authorship contribution statement

Prichard M. Tembo: Writing – original draft, Visualization, Methodology, Investigation, Formal analysis, Data curation. **Vaidyanathan Subramanian:** Writing – review & editing, Supervision, Resources, Methodology, Formal analysis, Conceptualization.

Declaration of competing interest

The authors declare the following financial interests/personal relationships which may be considered as potential competing interests: The authors declare that part of the work has been submitted as part of a patent application, Invention id: DIS22-23 Tech id: UNR22-017

Acknowledgements

The authors would like to acknowledge the National Science Foundation, which made this study possible through funds provided under grant number 2323629. The authors would also like to acknowledge the support of the Fulbright Foreign Student Program for their aid in making this study possible. We would also like to acknowledge Dr. E. Vahidi for providing access to analytical equipment which made the study possible. The authors would also like to acknowledge the assistance of Dr. C. Coronella in providing access to TGA equipment. The monetary support of the University of Nevada, Reno Department of Chemical and Materials Engineering for supporting undergraduate participation in this research, is greatly acknowledged. Lastly, the authors would like to acknowledge the contributions of the University of Nevada, Reno CHE440.640 Fall 2021 class in making this study a success through preliminary data acquisition and analysis.

Appendix A. Supplementary data

Supplementary data to this article can be found online at https://doi.org/10.1016/j.wmb.2024.08.007.

References

Aaltonen, M., Peng, C., Wilson, B.P., Lundström, M., 2017. Leaching of metals from spent lithium-ion batteries. Recycling 2 (4), 20. https://doi.org/10.3390/recycling2040020.

Aannir, M., Hakkou, R., Levard, C., Taha, Y., Ghennioui, A., Rose, J., Saadoune, I., 2023. Towards a closed loop recycling process of end-of-life lithium-ion batteries: Recovery of critical metals and electrochemical performance evaluation of a regenerated LiCoO2. J. Power Sources 580, 233341. https://doi.org/10.1016/j.jpowsour.2023.233341.

Abdalla, A.M., Abdullah, M.F., Dawood, M.K., Wei, B., Subramanian, Y., Azad, A.T., Nourin, S., Afroze, S., Taweekun, J., Azad, A.K., 2023. Innovative lithium-ion battery recycling: Sustainable process for recovery of critical materials from lithium-ion batteries. J. Energy Storage 67, 107551. https://doi.org/10.1016/j.est.2023.107551.

Amer, A., 2008. The hydrometallurgical extraction of lithium from Egyptian montmorillonite-type clay. JOM 60 (10), 55–57. https://doi.org/10.1007/s11837-008-0137-5.

Andrés, J.M., Ferrando, A.C., Membrado, L., 1996. Chemical desulfurization of coal with hydroiodic acid. Energy Fuels 10 (2), 425–430. https://doi.org/10.1021/ef9501612.

Barik, S., Prabaharan, G., Kumar, L., 2017. Leaching and separation of Co and Mn from electrode materials of spent lithium-ion batteries using hydrochloric acid: laboratory and pilot scale study. J. Clean. Prod. 147, 37–43. https://doi.org/10.1016/j.jclepro.2017.01.095.

Berckmans, G., Messagie, M., Smekens, J., Omar, N., Vanhaverbeke, L., Van Mierlo, J., 2017. Cost projection of state of the art lithium-ion batteries for electric vehicles up to 2030. Energies 10 (9), 1314. https://doi.org/10.3390/en10091314.

Beyer, M.K., Clausen-Schaumann, H., 2005. Mechanochemistry: the mechanical activation of covalent bonds. Chem. Rev. 105 (8), 2921–2948. https://doi.org/10.1021/cr030697h.

Bhandari, G.S., Dhawan, N., 2022. Investigation of hydrogen reduction for metal recovery from end-of-life lithium-ion batteries. J. Sustain. Metall. 8 (4), 1704–1718. https://doi.org/10.1007/s40831-022-00593-x.

Brownstein, S., Stillman, A., 1959. Proton resonance shifts of acids in liquid sulfur dioxide. J. Phys. Chem. 63 (12), 2061–2062.

Busch, M.A., 2018. Halogen Chemistry. Reference Module in Chemistry, Molecular Sciences and Chemical Engineering. Elsevier.

Castillo, S., Ansart, F., Laberty-Robert, C., Portal, J., 2002. Advances in the recovering of spent lithium battery compounds. J. Power Sources 112 (1), 247–254. https://doi.org/10.1016/S0378-7753(02)00361-0.

Cerrillo-Gonzalez, M.D.M., Villen-Guzman, M., Vereda-Alonso, C., Rodríguez-Maroto, J. M., Paz-Garcia, J.M., 2022. Acid leaching of LiCoO2 enhanced by reducing agent. Model formulation and validation. Chemosphere 287, 132020. https://doi.org/10.1016/j.chemosphere.2021.132020.

Chan, K.H., Anawati, J., Malik, M., Azimi, G., 2021. Closed-loop recycling of lithium, cobalt, nickel, and manganese from waste lithium-ion batteries of electric vehicles. ACS Sustain. Chem. Eng. 9 (12), 4398–4410. https://doi.org/10.1021/acssuschemeng.0c06869.

Chemanalyst, Hydrobromic Acid Price Trend and Forecast, 2024. https://www.chemanalyst.com/Pricing-data/hydrobromic-acid-1135 (accessed 30 July 2024).

Chemanalyst, Hydrochloric Acid Price Trend and Forecast, 2024. https://www.chemanalyst.com/Pricing-data/hydrochloric-acid-61 (accessed 30 July 2024).

Chen, J., Liu, J., Qi, Y., Sun, T., Li, X., 2013. Unveiling the roles of binder in the mechanical integrity of electrodes for lithium-ion batteries. J. Electrochem. Soc. 160 (9), A1502. https://doi.org/10.1149/2.088309jes.

Chu, H., Lie, J., Liu, J.-C., 2021. Rapid leaching of valuable metals from spent lithium-ion batteries with microwave irradiation using organic and inorganic acid. J. Sustain. Metall. 7 (2), 630–641. https://doi.org/10.1007/s40831-021-00362-2.

Dai, Y., Wang, N., Xu, Z., Gu, H., Chen, M., Hua, D., 2022. Acid-free leaching nickel, cobalt, manganese, and lithium from spent lithium-ion batteries using Fe (II) and Fe (III) solution. J. Sustain. Metall. 8 (2), 863–871. https://doi.org/10.1007/s40831-022-00530-y.

Degen, F., Winter, M., Bendig, D., Tübke, J., 2023. Energy consumption of current and future production of lithium-ion and post lithium-ion battery cells. Nat. Energy 8 (11), 1284–1295. https://doi.org/10.1038/s41560-023-01355-z.

Dickinson, C., Heal, G., 1999. Solid–liquid diffusion controlled rate equations. Thermochim. Acta 340, 89–103. https://doi.org/10.1016/S0040-6031(99)00256-7.

Duan, J., Tang, X., Dai, H., Yang, Y., Wu, W., Wei, X., Huang, Y., 2020. Building safe lithium-ion batteries for electric vehicles: a review. Electrochem. Energy Rev. 3 (1), 1–42. https://doi.org/10.1007/s41918-019-00060-4.

Dutta, D., Kumari, A., Panda, R., Jha, S., Gupta, D., Goel, S., Jha, M.K., 2018. Close loop separation process for the recovery of Co, Cu, Mn, Fe and Li from spent lithium-ion batteries. Sep. Purif. Technol. 200, 327–334. https://doi.org/10.1016/j.seppur.2018.02.022.

Espiari, S., Rashchi, F., Sadrnezhaad, S., 2006. Hydrometallurgical treatment of tailings with high zinc content. Hydrometallurgy 82 (1–2), 54–62. https://doi.org/10.1016/j.hydromet.2006.01.005.

Fan, X., Song, C., Lu, X., Shi, Y., Yang, S., Zheng, F., Huang, Y., Liu, K., Wang, H., Li, Q., 2021. Separation and recovery of valuable metals from spent lithium-ion batteries via concentrated sulfuric acid leaching and regeneration of LiNi1/3Co1/3Mn1/3O2. J. Alloys Compd. 863, 158775 https://doi.org/10.1016/j.jallcom.2021.158775.

Fan, E., Yang, J., Huang, Y., Lin, J., Arshad, F., Wu, F., Li, L., Chen, R., 2020. Leaching mechanisms of recycling valuable metals from spent lithium-ion batteries by a malonic acid-based leaching system. ACS Appl. Energy Mater. 3 (9), 8532–8542. https://doi.org/10.1021/acsaem.0c01166.

Gao, W., Zhang, X., Zheng, X., Lin, X., Cao, H., Zhang, Y., Sun, Z., 2017. Lithium carbonate recovery from cathode scrap of spent lithium-ion battery: a closed-loop process. Environ. Sci. Technol. 51 (3), 1662–1669. https://doi.org/10.1021/acs.est.6b03320.

Griskey, R.G., 2005. Transport Phenomena and Unit Operations: a Combined Approach. John Wiley & Sons.

Gu, K., Gu, X., Wang, Y., Qin, W., Han, J., 2023. A green strategy for recycling cathode materials from spent lithium-ion batteries using glutathione. Green Chem. 25 (11), 4362–4374. https://doi.org/10.1039/D3GC00540B.

Guimarães, L.F., Junior, A.B., Espinosa, D.C.R., 2022. Sulfuric acid leaching of metals from waste Li-ion batteries without using reducing agent. Miner. Eng. 183, 107597 https://doi.org/10.1016/j.mineng.2022.107597.

Guo, H., Kuang, G., Wang, H., Yu, H., Zhao, X., 2017. Investigation of enhanced leaching of lithium from α-spodumene using hydrofluoric and sulfuric acid. Minerals 7 (11), 205. https://doi.org/10.3390/min7110205.

Guo, H., Kuang, G., Wan, H., Yang, Y., Yu, H.-Z., Wang, H.-D., 2019. Enhanced acid treatment to extract lithium from lepidolite with a fluorine-based chemical method. Hydrometallurgy 183, 9–19. https://doi.org/10.1016/j.hydromet.2018.10.020.

Guo, Y., Li, F., Zhu, H., Li, G., Huang, J., He, W., 2016. Leaching lithium from the anode electrode materials of spent lithium-ion batteries by hydrochloric acid (HCl). Waste Manag. 51, 227–233. https://doi.org/10.1016/j.wasman.2015.11.036.

Hanisch, C., Loellhoeffel, T., Diekmann, J., Markley, K.J., Haselrieder, W., Kwade, A., 2015. Recycling of lithium-ion batteries: a novel method to separate coating and foil of electrodes. J. Clean. Prod. 108, 301–311. https://doi.org/10.1016/j.jclepro.2015.08.026.

Harper, G., Sommerville, R., Kendrick, E., Driscoll, L., Slater, P., Stolkin, R., Walton, A., Christensen, P., Heidrich, O., Lambert, S., 2019. Recycling lithium-ion batteries from electric vehicles. Nature 575 (7781), 75–86. https://doi.org/10.1038/s41586-019-1682-5.

He, L.-P., Sun, S.-Y., Mu, Y.-Y., Song, X.-F., Yu, J.-G., 2017. Recovery of lithium, nickel, cobalt, and manganese from spent lithium-ion batteries using L-tartaric acid as a leachant. ACS Sustain. Chem. Eng. 5 (1), 714–721. https://doi.org/10.1021/acssuschemeng.6b02056.

Huang, B., Pan, Z., Su, X., An, L., 2018. Recycling of lithium-ion batteries: Recent advances and perspectives. J. Power Sources 399, 274–286. https://doi.org/10.1016/j.jpowsour.2018.07.116.

Jha, M.K., Kumari, A., Jha, A.K., Kumar, V., Hait, J., Pandey, B.D., 2013. Recovery of lithium and cobalt from waste lithium ion batteries of mobile phone. Waste Manag. 33 (9), 1890–1897. https://doi.org/10.1016/j.wasman.2013.05.008.

Jung, Y., Yoo, B., Park, S., Kim, Y., Son, S., 2021. Study on roasting for selective lithium leaching of cathode active materials from spent lithium-ion batteries. Metals 11 (9), 1336. https://doi.org/10.3390/met11091336.

Ku, H., Jung, Y., Jo, M., Park, S., Kim, S., Yang, D., Rhee, K., An, E.-M., Sohn, J., Kwon, K., 2016. Recycling of spent lithium-ion battery cathode materials by ammoniacal leaching. J. Hazard. Mater. 313, 138–146. https://doi.org/10.1016/j.jhazmat.2016.03.062.

Lee, C.K., Rhee, K.-I., 2002. Preparation of LiCoO2 from spent lithium-ion batteries. J. Power Sources 109 (1), 17–21. https://doi.org/10.1016/S0378-7753(02)00037-X.

Lee, C.K., Rhee, K.-I., 2003. Reductive leaching of cathodic active materials from lithium ion battery wastes. Hydrometallurgy 68 (1–3), 5–10. https://doi.org/10.1016/S0304-386X(02)00167-6.

Li, H., Cormier, M., Zhang, N., Inglis, J., Li, J., Dahn, J.R., 2019. Is cobalt needed in Ni-rich positive electrode materials for lithium ion batteries? J. Electrochem. Soc. 166 (4), A429. https://doi.org/10.1149/2.1381902jes.

Li, L., Dunn, J.B., Zhang, X.X., Gaines, L., Chen, R.J., Wu, F., Amine, K., 2013. Recovery of metals from spent lithium-ion batteries with organic acids as leaching reagents

and environmental assessment. J. Power Sources 233, 180–189. https://doi.org/10.1016/j.jpowsour.2012.12.089.
Li, J., Shi, P., Wang, Z., Chen, Y., Chang, C.-C., 2009. A combined recovery process of metals in spent lithium-ion batteries. Chemosphere 77 (8), 1132–1136. https://doi.org/10.1016/j.chemosphere.2009.08.040.
Li, H., Xing, S., Liu, Y., Li, F., Guo, H., Kuang, G., 2017. Recovery of lithium, iron, and phosphorus from spent LiFePO4 batteries using stoichiometric sulfuric acid leaching system. ACS Sustain. Chem. Eng. 5 (9), 8017–8024. https://doi.org/10.1021/acssuschemeng.7b01594.
Liang, Z., Cai, C., Peng, G., Hu, J., Hou, H., Liu, B., Liang, S., Xiao, K., Yuan, S., Yang, J., 2021. Hydrometallurgical recovery of spent lithium ion batteries: environmental strategies and sustainability evaluation. ACS Sustain. Chem. Eng. 9 (17), 5750–5767. https://doi.org/10.1021/acssuschemeng.1c00942.
Lin, L., Lu, Z., Zhang, W., 2021. Recovery of lithium and cobalt from spent Lithium-Ion batteries using organic aqua regia (OAR): Assessment of leaching kinetics and global warming potentials. Resour. Conserv. Recycl. 167, 105416 https://doi.org/10.1016/j.resconrec.2021.105416.
Liu, C., Lin, J., Cao, H., Zhang, Y., Sun, Z., 2019. Recycling of spent lithium-ion batteries in view of lithium recovery: A critical review. J. Clean. Prod. 228, 801–813. https://doi.org/10.1016/j.jclepro.2019.04.304.
Lv, W., Wang, Z., Cao, H., Sun, Y., Zhang, Y., Sun, Z., 2018. A critical review and analysis on the recycling of spent lithium-ion batteries. ACS Sustain. Chem. Eng. 6 (2), 1504–1521. https://doi.org/10.1021/acssuschemeng.7b03811.
Maghsoudlou, M.S.A., Ebadzadeh, T., Sharafi, Z., Arabi, M., Zahabi, K.R., 2016. Synthesis and sintering of nano-sized forsterite prepared by short mechanochemical activation process. J. Alloys Compd. 678, 290–296. https://doi.org/10.1016/j.jallcom.2016.02.020.
Makuza, B., Tian, Q., Guo, X., Chattopadhyay, K., Yu, D., 2021. Pyrometallurgical options for recycling spent lithium-ion batteries: A comprehensive review. J. Power Sources 491, 229622. https://doi.org/10.1016/j.jpowsour.2021.229622.
Manjong, N.B., Marinova, S., Bach, V., Burheim, O.S., Finkbeiner, M., Strømman, A.H., 2024. Approaching battery raw material sourcing through a material criticality lens. Sustain. Prod. Consum. 49, 289–303. https://doi.org/10.1016/j.spc.2024.06.020.
Marscheider-Weidemann, F., Langkau, S., Baur, S.J., Billaud, M., Deubzer, O., Eberling, E., Erdmann, L., Haendel, M., Krail, M., Loibl, A., Maisel, F., Marwede, M., Neef, C., Neuwirth, M., Rostek, L., Rückschloss, J., Shirinzadeh, S., Stijepic, D., Tercero Espinoza, L., Tippner, M., 2021. Raw Materials for Emerging Technologies 2021. DERA Rohstoffinformationen 50 (348).
McGrath, M.J., Kuo, I.W., Ghogomu, J.N., Mundy, C.J., Marenich, A.V., Cramer, C.J., Truhlar, D.G., Siepmann, J.I., 2013. Calculation of the Gibbs free energy of solvation and dissociation of HCl in water via Monte Carlo simulations and continuum solvation models. Phys. Chem. Chem. Phys. 15 (32), 13578–13585. https://doi.org/10.1039/C3CP51762D.
Meshram, P., Pandey, B., Mankhand, T., 2015. Recovery of valuable metals from cathodic active material of spent lithium ion batteries: Leaching and kinetic aspects. Waste Manag. 45, 306–313. https://doi.org/10.1016/j.wasman.2015.05.027.
Meshram, P., Pandey, B., Mankhand, T., 2015. Hydrometallurgical processing of spent lithium ion batteries (LIBs) in the presence of a reducing agent with emphasis on kinetics of leaching. Chem. Eng. J. 281, 418–427. https://doi.org/10.1016/j.cej.2015.06.071.
Meshram, P., Abhilash, B.D., Pandey, T.R., Mankhand, H., 2016. Deveci, Comparision of different reductants in leaching of spent lithium ion batteries. JOM 68, 2613–2623. https://doi.org/10.1007/s11837-016-2032-9.
Mo, J.Y., Jeon, W., 2018. The impact of electric vehicle demand and battery recycling on price dynamics of lithium-ion battery cathode materials: A vector error correction model (VECM) analysis. Sustainability 10 (8), 2870. https://doi.org/10.3390/su10082870.
Musariri, B., Akdogan, G., Dorfling, C., Bradshaw, S., 2019. Evaluating organic acids as alternative leaching reagents for metal recovery from lithium ion batteries. Miner. Eng. 137, 108–117. https://doi.org/10.1016/j.mineng.2019.03.027.
Nadimi, H., Karazmoudeh, N.J., 2021. Selective separation and purification of Mn from Co and Ni in waste mobile phone Lithium-Ion batteries using D2EHAP via solvent extraction method. J. Sustain. Metall. 7 (2), 653–663. https://doi.org/10.1007/s40831-021-00371-1.
Nayl, A., Elkhashab, R., Badawy, S.M., El-Khateeb, M., 2017. Acid leaching of mixed spent Li-ion batteries. Arab. J. Chem. 10, S3632–S3639. https://doi.org/10.1016/j.arabjc.2014.04.001.
Peng, C., Hamuyuni, J., Wilson, B.P., Lundström, M., 2018. Selective reductive leaching of cobalt and lithium from industrially crushed waste Li-ion batteries in sulfuric acid system. Waste Manag. 76, 582–590. https://doi.org/10.1016/j.wasman.2018.02.052.
Philippot, M., Alvarez, G., Ayerbe, E., Van Mierlo, J., Messagie, M., 2019. Eco-efficiency of a lithium-ion battery for electric vehicles: Influence of manufacturing country and commodity prices on ghg emissions and costs. Batteries 5 (1), 23. https://doi.org/10.3390/batteries5010023.
Pinegar, H., Smith, Y.R., 2019. Recycling of end-of-life lithium ion batteries, Part I: commercial processes. J. Sustain. Metall. 5, 402–416. https://doi.org/10.1007/s40831-019-00235-9.
Porvali, A., Aaltonen, M., Ojanen, S., Velazquez-Martinez, O., Eronen, E., Liu, F., Wilson, B.P., Serna-Guerrero, R., Lundström, M., 2019. Mechanical and hydrometallurgical processes in HCl media for the recycling of valuable metals from Li-ion battery waste. Resour. Conserv. Recycl. 142, 257–266. https://doi.org/10.1016/j.resconrec.2018.11.023.
Quebec, P., 2019. Lithium-ion Battery Sector: Developing a Promising Sector for Quebec's Economy. KPMG for Propulsion Quebec, Montreal, QC Canada.
Riahi, K., Van Vuuren, D.P., Kriegler, E., Edmonds, J., O'neill, B.C., Fujimori, S., Bauer, N., Calvin, K., Dellink, R., Fricko, O., 2017. The Shared Socioeconomic Pathways and their energy, land use, and greenhouse gas emissions implications: An overview. Glob. Environ. Change 42, 153–168. https://doi.org/10.1016/j.gloenvcha.2016.05.009.
Rosales, G.D., Ruiz, M.C., Rodriguez, M.H., 2016. Study of the extraction kinetics of lithium by leaching β-spodumene with hydrofluoric acid. Minerals 6 (4), 98. https://doi.org/10.3390/min6040098.
Ryu, H.-H., Sun, H.H., Myung, S.-T., Yoon, C.S., Sun, Y.-K., 2021. Reducing cobalt from lithium-ion batteries for the electric vehicle era. Energy Environ. Sci. 14 (2), 844–852. https://doi.org/10.1039/d0ee03581e.
Saleem, U., Joshi, B., Bandyopadhyay, S., 2023. Hydrometallurgical routes to close the loop of electric vehicle (EV) lithium-ion batteries (LIBs) value chain: a review. J. Sustain Metall. 1–22. https://doi.org/10.1007/s40831-023-00718-w.
Seliverstov, V., 2016. Kinetic Fick's law and the integral-differential method of solving the neutron transport equation. At. Energy 120 (3), 153–164. https://doi.org/10.1007/s10512-016-0111-1.
Setiawan, H., Petrus, H.T.B.M., Perdana, I., 2019. Reaction kinetics modeling for lithium and cobalt recovery from spent lithium-ion batteries using acetic acid. Int. J. Miner. Metall. Mater. 26 (1), 98–107. https://doi.org/10.1007/s12613-019-1713-0.
Shuva, M.A.H., Kurny, A., 2013. Hydrometallurgical recovery of value metals from spent lithium ion batteries. Am. J. Mater. Eng. Technol. 1 (1), 8–12. https://doi.org/10.12691/materials-1-1-2.
Sigma-Aldrich, Hydriodic Acid Safety Data Sheet. Sigma-Aldrich 1-12. https://www.sigmaaldrich.com/US/en/sds/sial/58159, 2024 (accessed 23 July 2024).
Sigma-Aldrich, Hydrobromic Acid Safety Data Sheet. Sigma-Aldrich 1-10. https://www.sigmaaldrich.com/US/en/sds/sigald/339245, 2024 (accessed 23 July 2024).
Sitando, O., Crouse, P.L., 2012. Processing of a Zimbabwean petalite to obtain lithium carbonate. Int. J. Miner. Process. 102, 45–50. https://doi.org/10.1016/j.minpro.2011.09.014.
Sommerville, R., Shaw-Stewart, J., Goodship, V., Rowson, N., Kendrick, E., 2020. A review of physical processes used in the safe recycling of lithium ion batteries. SM&T 25, e00197.
Tan, Q., Li, J., 2015. Recycling metals from wastes: a novel application of mechanochemistry. Environ. Sci. Technol. 49 (10), 5849–5861. https://doi.org/10.1021/es506016w.
Tang, Y.-C., Wang, J.-Z., Shen, Y.-H., 2023. Separation of valuable metals in the recycling of lithium batteries via solvent extraction. Minerals 13 (2), 285. https://doi.org/10.3390/min13020285.
Tanong, K., Coudert, L., Chartier, M., Mercier, G., Blais, J.-F., 2017. Study of the factors influencing the metals solubilisation from a mixture of waste batteries by response surface methodology. Environ. Technol. 38 (24), 3167–3179. https://doi.org/10.1080/09593330.2017.1291756.
Tembo, P.M., Dyer, C., Subramanian, V., 2024. Lithium-ion battery recycling – A review of the material supply and policy infrastructure. NPG Asia Mater. 16 (43) https://doi.org/10.1038/s41427-024-00562-8.
Verma, A., Johnson, G.H., Corbin, D.R., Shiflett, M.B., 2020. Separation of lithium and cobalt from LiCoO2: a unique critical metals recovery process utilizing oxalate chemistry. ACS Sustain. Chem. Eng. 8 (15), 6100–6108. https://doi.org/10.1021/acssuschemeng.0c01128.
Vieceli, N., Nogueira, C.A., Guimarães, C., Pereira, M.F., Durão, F.O., Margarido, F., 2018. Hydrometallurgical recycling of lithium-ion batteries by reductive leaching with sodium metabisulphite. Waste Manag. 71, 350–361. https://doi.org/10.1016/j.wasman.2017.09.032.
Vieceli, N., Vonderstein, C., Swiontekc, T., Stopić, S., Dertmann, C., Sojka, R., Reinhardt, N., Ekberg, C., Friedrich, B., Petranikova, M., 2023. Recycling of Li-ion batteries from industrial processing: upscaled hydrometallurgical treatment and recovery of high purity manganese by solvent extraction. Solvent Extr. Ion Exc. 41 (2), 205–220. https://doi.org/10.1080/07366299.2023.2165405.
Vishvakarma, S., Dhawan, N., 2019. Recovery of cobalt and lithium values from discarded Li-ion batteries. J. Sustain. Metall. 5, 204–209. https://doi.org/10.1007/s40831-018-00208-4.
Vu, H., Bernardi, J., Jandová, J., Vaculíková, L., Goliáš, V., 2013. Lithium and rubidium extraction from zinnwaldite by alkali digestion process: Sintering mechanism and leaching kinetics. Int. J. Miner. Process. 123, 9–17. https://doi.org/10.1016/j.minpro.2013.04.014.
Wang, R.-C., Lin, Y.-C., Wu, S.-H., 2009. A novel recovery process of metal values from the cathode active materials of the lithium-ion secondary batteries. Hydrometallurgy 99 (3–4), 194–201. https://doi.org/10.1016/j.hydromet.2009.08.005.
Wang, F., Sun, R., Xu, J., Chen, Z., Kang, M., 2016. Recovery of cobalt from spent lithium ion batteries using sulphuric acid leaching followed by solid–liquid separation and solvent extraction. RSC Adv. 6 (88), 85303–85311. https://doi.org/10.1039/C6RA16801A.
Wang, M., Tan, Q., Li, J., 2018. Unveiling the role and mechanism of mechanochemical activation on lithium cobalt oxide powders from spent lithium-ion batteries. Environ. Sci. Technol. 52 (22), 13136–13143. https://doi.org/10.1021/acs.est.8b03469.
Wei, Q., Xiong, F., Tan, S., Huang, L., Lan, E.H., Dunn, B., Mai, L., 2017. Porous one-dimensional nanomaterials: design, fabrication and applications in electrochemical energy storage. Adv. Mater. 29 (20), 1602300 https://doi.org/10.1002/adma.201602300.
Westmoreland, P., 1993. Elements of chemical engineering: by H. Scott Fogler. Chem. Eng. Educ. 27 (4), 161–167.
Wu, C., Li, B., Yuan, C., Ni, S., Li, L., 2019. Recycling valuable metals from spent lithium-ion batteries by ammonium sulfite-reduction ammonia leaching. Waste Manag. 93, 153–161. https://doi.org/10.1016/j.wasman.2019.04.039.

Xing, L., Bao, J., Zhou, S., Qiu, Y., Sun, H., Gu, S., Yu, J., 2021. Ultra-fast leaching of critical metals from spent lithium-ion batteries cathode materials achieved by the synergy-coordination mechanism. Chem. Eng. J. 420, 129593 https://doi.org/10.1016/j.cej.2021.129593.

Xu, M., Kang, S., Jiang, F., Yan, X., Zhu, Z., Zhao, Q., Teng, Y., Wang, Y., 2021. A process of leaching recovery for cobalt and lithium from spent lithium-ion batteries by citric acid and salicylic acid. RSC Adv. 11 (44), 27689–27700. https://doi.org/10.1039/D1RA04979H.

Xu, J., Thomas, H., Francis, R.W., Lum, K.R., Wang, J., Liang, B., 2008. A review of processes and technologies for the recycling of lithium-ion secondary batteries. J. Power Sources 177 (2), 512–527. https://doi.org/10.1016/j.jpowsour.2007.11.074.

Xuan, W., de Souza Braga, A., Korbel, C., Chagnes, A., 2021. New insights in the leaching kinetics of cathodic materials in acidic chloride media for lithium-ion battery recycling. Hydrometallurgy 204, 105705. https://doi.org/10.1016/j.hydromet.2021.105705.

W. Xuan, A. Otsuki, A. Chagnes, Investigation of the leaching mechanism of NMC 811 (LiNi 0.8 Mn 0.1 Co 0.1 O 2) by hydrochloric acid for recycling lithium ion battery cathodes. RSC Adv. 9 (66) (2019) 38612-38618. doi: 10.1039/C9RA06686A.

Yadav, P., Jie, C.J., Tan, S., Srinivasan, M., 2020. Recycling of cathode from spent lithium iron phosphate batteries. J. Hazard. Mater. 399, 123068 https://doi.org/10.1016/j.jhazmat.2020.123068.

Yan, Q., Li, X., Yin, Z., Wang, Z., Guo, H., Peng, W., Hu, Q., 2012. A novel process for extracting lithium from lepidolite. Hydrometallurgy 121, 54–59. https://doi.org/10.1016/j.hydromet.2012.04.006.

Yang, Y., Xu, S., He, Y., 2017. Lithium recycling and cathode material regeneration from acid leach liquor of spent lithium-ion battery via facile co-extraction and co-precipitation processes. Waste Manag. 64, 219–227. https://doi.org/10.1016/j.wasman.2017.03.018.

Yang, Y., Zheng, X., Cao, H., Zhao, C., Lin, X., Ning, P., Zhang, Y., Jin, W., Sun, Z., 2017. A closed-loop process for selective metal recovery from spent lithium iron phosphate batteries through mechanochemical activation. ACS Sustain. Chem. Eng. 5 (11), 9972–9980. https://doi.org/10.1021/acssuschemeng.7b01914.

Yao, L., Feng, Y., Xi, G., 2015. A new method for the synthesis of LiNi 1/3 Co 1/3 Mn 1/3 O 2 from waste lithium ion batteries. RSC Adv. 5 (55), 44107–44114. https://doi.org/10.1039/C4RA16390G.

Yao, Y., Zhu, M., Zhao, Z., Tong, B., Fan, Y., Hua, Z., 2018. Hydrometallurgical processes for recycling spent lithium-ion batteries: a critical review. ACS Sustain. Chem. Eng. 6 (11), 13611–13627. https://doi.org/10.1021/acssuschemeng.8b03545.

Yu, X., Li, W., Gupta, V., Gao, H., Tran, D., Sarwar, S., Chen, Z., 2022. Current challenges in efficient lithium-ion batteries' recycling: A perspective. Glob. Chall. 6 (12), 2200099. https://doi.org/10.1002/gch2.202200099.

Yue, Y., Wei, S., Yongjie, B., Chenyang, Z., Shaole, S., Yuehua, H., 2018. Recovering valuable metals from spent lithium ion battery via a combination of reduction thermal treatment and facile acid leaching. ACS Sustain. Chem. Eng. 6 (8), 10445–10453. https://doi.org/10.1021/acssuschemeng.8b01805.

Zhang, X., Bian, Y., Xu, S., Fan, E., Xue, Q., Guan, Y., Wu, F., Li, L., Chen, R., 2018. Innovative application of acid leaching to regenerate Li (Ni1/3Co1/3Mn1/3) O2 cathodes from spent lithium-ion batteries. ACS Sustain. Chem. Eng. 6 (5), 5959–5968. https://doi.org/10.1021/acssuschemeng.7b04373.

Zhang, X., Li, L., Fan, E., Xue, Q., Bian, Y., Wu, F., Chen, R., 2018. Toward sustainable and systematic recycling of spent rechargeable batteries. Chem. Soc. Rev. 47 (19), 7239–7302. https://doi.org/10.1039/C8CS00297E.

Zhao, J., Zhang, B., Xie, H., Qu, J., Qu, X., Xing, P., Yin, H., 2020. Hydrometallurgical recovery of spent cobalt-based lithium-ion battery cathodes using ethanol as the reducing agent. Environ. Res. 181, 108803 https://doi.org/10.1016/j.envres.2019.108803.

Zheng, X., Gao, W., Zhang, X., He, M., Lin, X., Cao, H., Zhang, Y., Sun, Z., 2017. Spent lithium-ion battery recycling–Reductive ammonia leaching of metals from cathode scrap by sodium sulphite. Waste Manag. 60, 680–688. https://doi.org/10.1016/j.wasman.2016.12.007.

Zheng, Y., Song, W., Mo, W.-T., Zhou, L., Liu, J.-W., 2018. Lithium fluoride recovery from cathode material of spent lithium-ion battery. RSC Adv. 8 (16), 8990–8998. https://doi.org/10.1039/C8RA00061A.

Zhou, M., Li, B., Li, J., Xu, Z., 2021. Pyrometallurgical technology in the recycling of a spent lithium ion battery: evolution and the challenge. ACS ES&T Eng. 1 (10), 1369–1382. https://doi.org/10.1021/acsestengg.1c00067.

Zhou, L., Zhang, K., Hu, Z., Tao, Z., Mai, L., Kang, Y.M., Chou, S.L., Chen, J., 2018. Recent developments on and prospects for electrode materials with hierarchical structures for lithium-ion batteries. Adv. Energy Mater. 8 (6), 1701415 https://doi.org/10.1002/aenm.201701415.

Zhu, S.-G., He, W.-Z., Li, G.-M., Xu, Z., Zhang, X.-J., Huang, J.-W., 2012. Recovery of Co and Li from spent lithium-ion batteries by combination method of acid leaching and chemical precipitation. T. Nonferr. Metal. Soc. 22 (9), 2274–2281. https://doi.org/10.1016/S1003-6326(11)61460-X.

Ziegler, M.S., Trancik, J.E., 2021. Re-examining rates of lithium-ion battery technology improvement and cost decline. Energy Environ. Sci. 14 (4), 1635–1651. https://doi.org/10.1039/D0EE02681F.

Ziegler, M.S., Song, J., Trancik, J.E., 2021. Determinants of lithium-ion battery technology cost decline. Energy Environ. Sci. https://doi.org/10.1039/D1EE01313K.

Zou, H., Gratz, E., Apelian, D., Wang, Y., 2013. A novel method to recycle mixed cathode materials for lithium ion batteries. Green Chem. 15 (5), 1183–1191. https://doi.org/10.1039/C3GC40182K.

Zumdahl, S.S., DeCoste, D.J., 2012. Chemical Principles. Cengage Learning.